








OPEN ACCESS

Original research

# Genetics impact risk of Alzheimer's disease through mechanisms modulating structural brain morphology in late life

Roxanna Korologou-Linden <sup>1,2</sup> Bing Xu,<sup>3,4</sup> Elizabeth Coulthard <sup>5,6</sup>, Esther Walton,<sup>1,7</sup> Alfie Wearn <sup>5</sup> Gibran Hemani,<sup>1,2</sup> Tonya White,<sup>3,8</sup> Charlotte Cecil,<sup>9</sup> Tamsin Sharp,<sup>1,10</sup> Henning Tiemeier,<sup>4,11</sup> Tobias Banaschewski,<sup>12</sup> Arun Bokde <sup>13</sup>, Sylvane Desrivieres,<sup>14</sup> Herta Flor,<sup>15,16</sup> Antoine Grigis,<sup>17</sup> Hugh Garavan,<sup>18</sup> Penny Gowland,<sup>19</sup> Andreas Heinz,<sup>20</sup> Rüdiger Brühl,<sup>21</sup> Jean-Luc Martinot,<sup>22,23</sup> Marie-Laure Paillère Martinot,<sup>22,23</sup> Eric Artiges,<sup>22,23</sup> Frauke Nees,<sup>12,15,24</sup> Dimitri Papadopoulos Orfanos,<sup>25</sup> Tomáš Paus,<sup>26,27</sup> Luise Poustka,<sup>28</sup> Sabina Millenet,<sup>12</sup> Juliane H Fröhner,<sup>29</sup> Michael Smolka,<sup>29</sup> Henrik Walter,<sup>30,31</sup> Jeanne Winterer,<sup>20,32</sup> Robert Whelan,<sup>33</sup> Gunter Schumann,<sup>14,34,35</sup> Laura D Howe,<sup>1,2</sup> Yoav Ben-Shlomo,<sup>2</sup> Neil M Davies,<sup>1,2,36</sup> Emma Louise Anderson <sup>1,2,36</sup>

► Additional supplemental material is published online only. To view, please visit the journal online (<https://doi.org/10.1136/jnnp-2023-332969>).

For numbered affiliations see end of article.

## Correspondence to

Dr Roxanna Korologou-Linden, Medical Research Council Integrative Epidemiology Unit, University of Bristol, Bristol, BS8 1QU, UK; [rk17685@bristol.ac.uk](mailto:rk17685@bristol.ac.uk)

NMD and ELA contributed equally.

Received 9 November 2023  
Accepted 11 March 2024



© Author(s) (or their employer(s)) 2024. Re-use permitted under CC BY. Published by BMJ.

**To cite:** Korologou-Linden R, Xu B, Coulthard E, *et al.* *J Neurol Neurosurg Psychiatry* Epub ahead of print: [please include Day Month Year]. doi:10.1136/jnnp-2023-332969

## ABSTRACT

**Background** Alzheimer's disease (AD)-related neuropathological changes can occur decades before clinical symptoms. We aimed to investigate whether neurodevelopment and/or neurodegeneration affects the risk of AD, through reducing structural brain reserve and/or increasing brain atrophy, respectively.

**Methods** We used bidirectional two-sample Mendelian randomisation to estimate the effects between genetic liability to AD and global and regional cortical thickness, estimated total intracranial volume, volume of subcortical structures and total white matter in 37 680 participants aged 8–81 years across 5 independent cohorts (Adolescent Brain Cognitive Development, Generation R, IMAGEN, Avon Longitudinal Study of Parents and Children and UK Biobank). We also examined the effects of global and regional cortical thickness and subcortical volumes from the Enhancing Neuroimaging Genetics through Meta-Analysis (ENIGMA) Consortium on AD risk in up to 37 741 participants.

**Results** Our findings show that AD risk alleles have an age-dependent effect on a range of cortical and subcortical brain measures that starts in mid-life, in non-clinical populations. Evidence for such effects across childhood and young adulthood is weak. Some of the identified structures are not typically implicated in AD, such as those in the striatum (eg, thalamus), with consistent effects from childhood to late adulthood. There was little evidence to suggest brain morphology alters AD risk.

**Conclusions** Genetic liability to AD is likely to affect risk of AD primarily through mechanisms affecting indicators of brain morphology in later life, rather than structural brain reserve. Future studies with repeated measures are required for a better understanding and certainty of the mechanisms at play.

## INTRODUCTION

The earliest Alzheimer's disease (AD)-related histopathological changes are typically observed within

## WHAT IS ALREADY KNOWN ON THIS TOPIC

- ⇒ Little is known about the dynamic interplay between brain morphology and Alzheimer's disease throughout the life course.
- ⇒ Most prior research has predominantly focused on overall brain structure metrics, such as estimated total intracranial volume, mean thickness and total surface area.

## WHAT THIS STUDY ADDS

- ⇒ This is the first bidirectional Mendelian randomisation study to assess the effects between Alzheimer's disease, and both global and regional measurements of cortical thickness, estimated total intracranial volume, total white matter and subcortical structure volumes, using different cohorts spanning the life course.

## HOW THIS STUDY MIGHT AFFECT RESEARCH, PRACTICE OR POLICY

- ⇒ Brain morphology is likely to play a role in changing the risk of Alzheimer's disease through neurodegenerative pathways such as a loss of brain matter, rather than neurodevelopmental pathways such as building brain reserve.
- ⇒ Future research should focus efforts on using different measures of structural and functional brain morphology, starting in mid-adulthood.

the medial temporal lobes and disperse throughout the frontal, parietal and temporal neocortices and subcortical regions by the time a clinical diagnosis of AD is made.<sup>1</sup> Amyloid- $\beta$  accumulation in the brain may be apparent 20 years before the appearance of clinical symptoms.<sup>2</sup> Hence, the integration of biological data prior to the onset of clinical

symptoms is crucial in understanding the aetiology, timing and progression of the disease, and for the development of more efficient strategies for early detection and screening of individuals for AD risk.

It has been argued that variability in AD risk may be mediated through both morphology ('brain reserve') and/or functional capacity to compensate for pathology ('cognitive reserve'),<sup>3</sup> which may operate independently or synergistically. Consequently, it has been hypothesised that genetic risk for AD may be mediated through determining the underlying brain reserve of an individual.<sup>4-6</sup> Furthermore, the relationship between brain structures and AD may be bidirectional, as genes associated with brain morphology (such as thickness and surface area) have been shown to be involved in neurogenesis.<sup>7</sup>

Genetic instruments allow for the identification of factors that modify disease risk, establish effects of prodromal disease and can help us discover biomarkers that predict disease. Genome-wide association studies (GWAS)<sup>8-11</sup> for AD have identified approximately 30 single nucleotide polymorphisms (SNPs), each with a modest effect on the risk of AD, apart from the  $\epsilon 4$  genotype in the *APOE* gene, whereby carriers may have up to 12-fold increased risk.<sup>11</sup> Previous studies examining the association of genetic liability to AD with brain morphology have typically used polygenic risk scores (PRS) at liberal thresholds, which can increase bias due to horizontal pleiotropy.<sup>6 12 13</sup> They also have small sample sizes, as genetic and neuroimaging data are rarely available in combination. Furthermore, SNPs associated with brain structure have been discovered using larger sample sizes<sup>7 14</sup> than previous neuroimaging studies,<sup>15 16</sup> allowing for the bidirectional investigation of the causal effects of structural brain measures on risk of AD, using Mendelian randomisation (MR). MR is a form of instrumental variable analysis which uses SNPs as instruments for exposures to estimate lifetime effects of phenotypes on disease risk (and vice versa).<sup>17</sup>

We investigated how genetic liability to AD affects brain morphology across the life course (from ages 8 to 81 years) using two-sample MR. This approach examines whether AD genetic susceptibility affects brain development or degeneration. Using two-sample MR, we also investigated whether brain morphology has a causal effect on the risk of AD, to establish whether greater thickness/volume provides a protective effect against advancing neuropathology and thus, reduces risk of an AD diagnosis ('brain reserve' hypothesis).

## MATERIALS AND METHODS

### Data

#### Alzheimer's disease GWAS

We extracted SNPs from the largest GWAS of clinically diagnosed AD,<sup>9</sup> which identified 27 SNPs to be associated with AD

risk in participants of European ancestry. For each SNP, we used the effect estimates from the stage with the largest sample size ( $n=82\,771$  to  $94\,437$  participants).

#### Brain structure GWAS

We used GWAS of brain structures (average thickness of 34 gyral-based cortical regions of interest, mean thickness, estimated total intracranial volume (eTIV), 9 subcortical volumes and the total volume of white matter) conducted within different cohorts across the life course. Regional thickness has been used to differentiate between mild cognitive impairment and individuals with AD with excellent accuracy, specificity and reproducibility across independent cohorts.<sup>18</sup> We conducted all GWAS described, except for the GWAS in the ENIGMA consortium which has been previously published.<sup>7 14 19 20</sup> GWAS for regional cortical thickness and subcortical volumes were adjusted for global cortical thickness and eTIV, respectively. For the peri-pubertal period, we used Generation R,<sup>21 22</sup> the Adolescent Brain Cognitive Development study (ABCD)<sup>23 24</sup> and IMAGEN.<sup>25</sup> For early adulthood, we meta-analysed the Avon Longitudinal Study of Parents and Children (ALSPAC)<sup>26-28</sup> and the second wave of data collection for the IMAGEN study.<sup>25</sup> For adulthood, we used the UK Biobank (UKB)<sup>29</sup> and stratified the sample into three equal-sized age tertiles, to examine age-specific effects (figures 1 and 2 and table 1). Finally, we used summary data from ENIGMA<sup>7 14</sup> ( $n=37\,741$  participants, age range 3.4–91.4 years), which includes the first release of UKB imaging data. All GWAS in the analyses were conducted in participants of European ancestry. Details of the cohorts, including the genotyping and neuroimaging procedures, are provided in online supplemental tables 1 and 2, respectively.

#### Statistical analyses

##### Estimating the causal effect of genetic liability to Alzheimer's disease on brain structures

###### Two-sample Mendelian randomisation

Two-sample MR is an extension of MR,<sup>30</sup> where the SNP effects on the exposure and on the outcome are extracted from separate GWAS studies. To examine the effects of genetic liability to AD on structural brain measures, we extracted SNPs strongly associated with AD ( $p \leq 5 \times 10^{-8}$ ).<sup>9</sup> Where SNPs were not available, we used proxy SNPs ( $r^2 > 0.80$ ). SNPs were clumped using  $r^2 > 0.001$  and a physical distance of 10 000 kb. We also included rs7412 and rs423958 to tag the *APOE*  $\epsilon 4$  allele. We used 23–25 SNPs as instruments for AD, the number varying by availability within each cohort (table 1). We harmonised the AD and brain structure GWAS in IMAGEN, Generation R, ABCD, ALSPAC and the UKB (online supplemental methods).

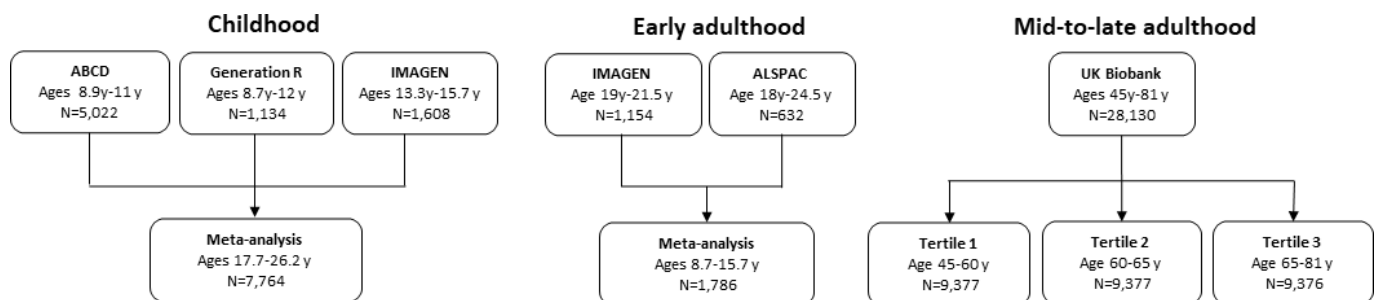


**Figure 1** Study cohorts in the age-stratified analysis of genetic liability to Alzheimer's disease on brain morphology. ABCD, Adolescent Brain Cognitive Development; ALSPAC Avon Longitudinal Study of Parents and Children; y, years.

## A Mendelian randomization of Alzheimer's disease genetic liability on structural brain morphology



## B Mendelian randomization of structural brain morphology on risk of Alzheimer's disease

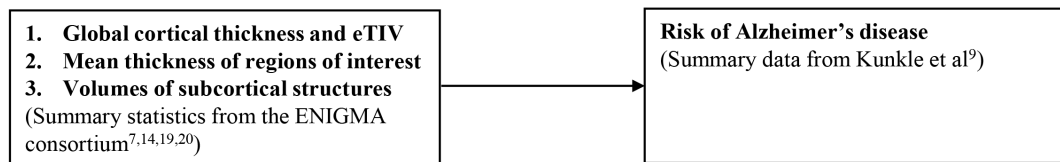


**Figure 2** Study design for examining the bidirectional effects between Alzheimer's disease and brain morphology. (A) Mendelian randomisation of Alzheimer's disease genetic liability on structural brain morphology. (B) Mendelian randomisation of structural brain morphology on risk of Alzheimer's disease. eTIV, estimated total intracranial volume.

We then employed univariable MR to estimate the effect of the AD SNPs on 9 subcortical volumes and the 34 cortical regions defined by the Desikan-Killiany atlas<sup>31</sup> (as well as total volume of white matter where available) within each cohort. We used a random-effects inverse-variance weighted (IVW) regression analysis, which assumes no directional horizontal pleiotropy<sup>17</sup> and used the F-statistic as a measure of instrument strength.<sup>32</sup> All effect estimates reflect SD changes in the outcome per doubling of genetic liability to AD.<sup>33</sup> Using the metagen function,<sup>34</sup> we applied random-effects models to meta-analyse the effects of the AD SNPs on structural brain measures for the three peri-pubertal cohorts: IMAGEN, ABCD and Generation R (figures 1 and 2). To examine how the age-level covariate was associated with the causal effect estimates across the three age-stratified tertiles of UKB, we extracted a p for trend across these groups, using the meta regress command in STATA V.16<sup>35</sup> and using the mean age of each tertile as the exposure. Sample sizes differed by brain structure due to quality control and missing data.

## Estimating the causal effect of brain structures on risk of Alzheimer's disease

## Two-sample Mendelian randomisation

Using the ENIGMA GWAS,<sup>7 14 19 20</sup> we extracted SNPs associated with eight subcortical volumes and the thickness of the regions of interest as defined by the Desikan-Killiany atlas.<sup>31</sup> The same parameters and harmonisation methods were used as in the previous analysis. Again, we employed univariable MR to examine the causal effects of each brain structure on risk of AD using a random-effects IVW regression. All effect estimates represent an OR for AD per SD increase in thickness or volume. There is overlap between ENIGMA and some of the individual-level cohorts. However, it has been shown that sample overlap results in little bias in the presence of strong instruments (ie,  $F > 10$ ).<sup>36</sup>

## Sensitivity analyses

We conducted sensitivity analyses to examine for potential violation of key MR assumptions. For MR to generate unbiased causal effect estimates, each genetic variant that is used as an instrumental variable must satisfy three assumptions: (1) that it is associated with the exposure (relevance assumption), (2) that it is not associated with the outcome through a confounding

**Table 1** Descriptive statistics of the cohorts used in the analysis

Cohort	N	Number of Alzheimer's disease SNPs	F-statistic for Alzheimer's disease SNPs	Mean age (SD)	Age range	% female
Childhood						
ABCD	5022	25	223.28	9.91 (0.6)	8.9–11	52.6
Generation R	1134	23	239.34	10.2 (0.6)	8.9–12	49.2
IMAGEN	1151–1154	23	224.67	14.4 (0.4)	13.3–15.7	50.6
Early adulthood						
ALSPAC	358–632	25	231.7	20.5 (1.6)	18–24.5	22.4
IMAGEN	1577–1608	23	224.7	26.2 (0.7)	17.7–26.2	51.3
Adulthood						
UK Biobank tertile 1	9377	24	231.5	55 (3.4)	45–60	57.0
UK Biobank tertile 2	9377	24	231.5	64.3 (2.2)	60–68	53.7
UK Biobank tertile 3	9376	24	231.5	72.0 (2.9)	68–81	46.0

ABCD, Adolescent Brain Cognitive Development; ALSPAC, Avon Longitudinal Study of Parents and Children; SNP, single nucleotide polymorphism.

pathway (exchangeability assumption) and (3) is only associated with the outcome through the exposure (exclusion restriction assumption). IVW regression assumes no horizontal pleiotropy and provides unbiased causal effect estimates only when there is balanced or no horizontal pleiotropy. We compared estimates from IVW with those from Egger regression,<sup>37, 38</sup> weighted median<sup>39</sup> and weighted mode,<sup>40</sup> which relax this assumption. Heterogeneity in the causal estimates was assessed using Cochran's Q-statistic.<sup>37</sup> Furthermore, to exclude the possibility that the SNPs used to proxy for AD are instruments for brain structures and vice versa, we performed a directionality (Steiger) test.<sup>41</sup> Where the hypothesised direction was false, we performed sensitivity analyses removing SNPs explaining more variance in the outcome than the exposure (details in online supplemental methods). Lastly, we excluded the two SNPs in the *APOE* locus from the AD instrument, to investigate whether the effects observed are primarily driven by the variants in the *APOE* gene. This study involves evaluating global patterns of effect estimates; hence, we focus on effect size and precision.<sup>42, 43</sup> Adjusted p values, controlling for the false discovery rate are in provided online supplemental tables 4, 8, 9 and 11.

## RESULTS

We used bidirectional two-sample MR<sup>30</sup> to first examine the effect of genetic liability to AD ( $p \leq 5 \times 10^{-8}$ ) on global and regional cortical thickness, eTIV, volumes of subcortical structures. We also included total white matter as an outcome where available. To boost the statistical power of the smaller childhood cohorts, we meta-analysed the causal effect estimates across ABCD,<sup>23, 24</sup> Generation R<sup>44, 45</sup> and IMAGEN<sup>25</sup> (aged 8–16 years). For early adulthood, we used participants selected for neuroimaging in ALSPAC substudies<sup>46</sup> (aged 18–24.5 years). For mid-to-late adulthood, we stratified the UKB population into three age tertiles: 45–60 years, 60–68 years and 68–81 years. In total, we used 23–25 independent AD SNPs from the largest GWAS of clinically diagnosed AD,<sup>9</sup> depending how many were available in each cohort used (table 1). Second, we examined the causal effects of brain morphology on AD risk, using genetic instruments for each brain structure from the ENIGMA consortium GWAS. A summary of our study design is presented in figures 1 and 2.

Of the 34 cortical regions and 10 subcortical structures examined, there was evidence to suggest that genetic liability to AD has an age-dependent effect on the thickness and volume of these measures, respectively, across mid-to-late adulthood, but the evidence for such effects in childhood through young adulthood is weak. When we examined the causal effects of the thickness of 27 cortical regions (ie, those regions with genetic variants at  $5 \times 10^{-8}$ ), we found little evidence of an effect of greater thickness on risk of AD. We only found evidence that hippocampal volume and thickness of lateral orbitofrontal and rostral anterior cingulate cortices affected AD risk. An overview of the findings is shown in table 2.

### Causal effects of genetic liability to Alzheimer's disease on brain structures

#### Childhood

Only weak evidence supported the association between genetic liability to AD and cortical thickness or subcortical volumes in school-aged children. A doubling in odds of genetic liability to AD was associated with a  $-0.02$  SD (95% CI  $-0.04$  to  $-0.01$ ) smaller volume of the thalamus (Braak stage IV) (figure 3A) and  $-0.03$  SD (95% CI  $-0.05$  to  $-0.01$ ) lower thickness of the

**Table 2** Summary of main findings

Exposure	Outcome	Timepoint	Direction
Genetic liability to Alzheimer's disease	Caudal anterior cingulate	Childhood	↓
	Thalamus		↓
	Thalamus	Early adulthood	↓
	Cuneus	Adulthood (45–60 years)	↑
	Inferior temporal		↑
	Accumbens	Adulthood (60–68 years)	↓
	Caudal middle frontal		↓
	Caudate		↓
	Putamen		↓
	Thalamus		↓
	Accumbens*	Adulthood (68–81 years)	↓
	Amygdala*		↓
	Caudate		↓
	Entorhinal*		↓
	Fusiform		↓
	Hippocampus*		↓
	Inferior temporal		↓
	Lateral occipital		↑
	Lateral ventricles		↑
	Middle temporal*		↓
Parahippocampal		↓	
Pericalcarine		↑	
Postcentral		↑	
Precentral		↑	
Superior parietal		↑	
Thalamus*		↓	
Transverse temporal		↑	
Hippocampus	Alzheimer's disease	Across the life course (summary data)	↑

Only analyses where 95% CIs show some evidence of association are displayed.  
\*Indicates  $p < 0.05$  following correction for multiple testing.

caudal anterior cingulate (Braak stage IV) (figure 3A, online supplemental tables 1–4).

#### Early adulthood

There was little evidence to suggest that a higher genetic liability to AD is associated with cortical regions and subcortical structures. However, a doubling in odds of genetic liability to AD was weakly associated with a  $-0.03$  lower thalamic volume (Braak stage IV) (figure 3A, online supplemental table 8) (SD  $-0.03$ ; 95% CI  $-0.06$  to  $-0.004$ ).

#### Mid-life to late life

We identified evidence of an age-dependent effect of AD genetic liability on smaller volume of the hippocampus (Braak stage II), accumbens (Braak stage II), amygdala (Braak stage II) and thalamus (Braak stage IV) (p for trend across age tertiles for each respective structure:  $1.32 \times 10^{-5}$ , 0.001, 0.02 and 0.03; online supplemental tables 9 and 10). Furthermore, we found evidence of age-dependent effect of AD genetic liability on lower thickness of the inferior temporal and middle temporal cortices (p for trend across age tertiles = 0.001 and  $p = 0.009$ , respectively; Braak stage IV, figure 3A). A doubling in odds of genetic liability to AD, for example, was associated with 0.02 SD (95% CI  $-0.04$  to  $-0.01$ ) lower thickness in the middle temporal cortex for participants of aged 68–81 years and a trend in the same direction was observed for participants aged 60–68 years. On the contrary,



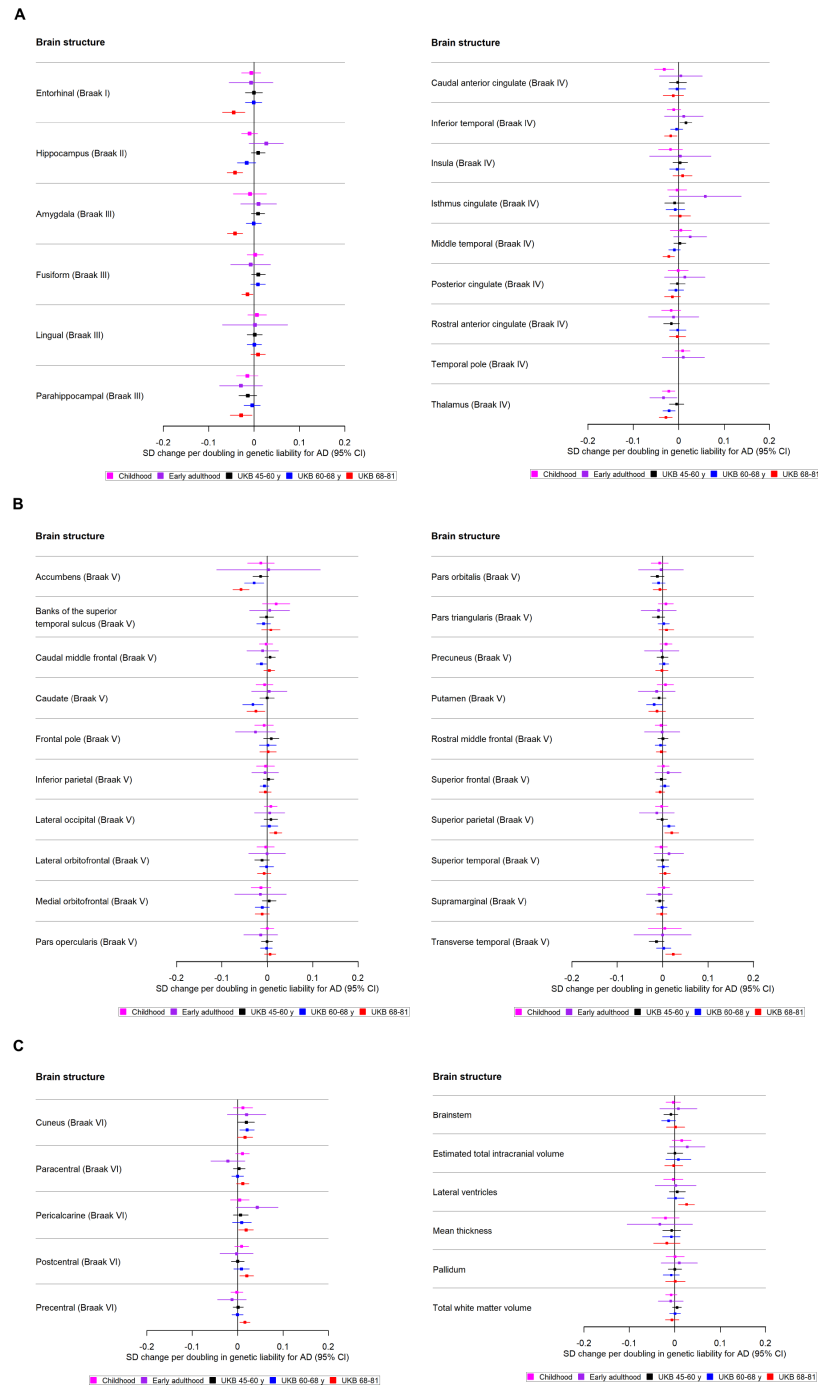


**Figure 3** (A) The causal effects of genetic liability to AD on brain structures in Braak stages I–IV at different ages across the life course (see figure 3B for structures in Braak stage V and figure 3C for Braak stage VI). The childhood cohorts include meta-analysed effects of three peri-pubertal cohorts: ABCD, GEN R and IMAGEN. The early adulthood cohort includes ALSPAC and the later adulthood cohorts include UKB. Effect estimates for cortical regions and subcortical structures represent SD changes in thickness and volume. Cortical regions were adjusted for mean thickness and subcortical volumes were adjusted for estimated intracranial volume. Where an effect estimate is missing, that structural measure was not available in that cohort. (B) The causal effects of genetic liability to AD on brain structures in Braak stages V at different ages across the life course (see figure 3C for structures in Braak stage VI). The childhood cohorts include meta-analysed effects of three peri-pubertal cohorts: ABCD, GEN R and IMAGEN. The early adulthood cohort includes ALSPAC and the later adulthood cohorts include UKB. Effect estimates for cortical regions and subcortical structures represent SD changes in thickness and volume. Cortical regions were adjusted for mean thickness and subcortical volumes were adjusted for estimated intracranial volume. Where an effect estimate is missing, that structural measure was not available in that cohort. (C) The causal effects of genetic liability to AD on brain structures in Braak stage VI, and those not included in Braak staging, at different ages across the life course. The childhood cohorts include meta-analysed effects of three peri-pubertal cohorts: ABCD, GEN R and IMAGEN. The early adulthood cohort includes ALSPAC and the later adulthood cohorts include UKB. Effect estimates for cortical regions and subcortical structures represent SD changes in thickness and volume. Cortical regions were adjusted for mean thickness, subcortical structures and volume of cerebral white matter were adjusted for estimated intracranial volume. Where an effect estimate is missing, that structural measure was not available in that cohort. ABCD, Adolescent Brain Cognitive Development; AD, Alzheimer's disease; ALSPAC, Avon Longitudinal Study of Parents and Children; GEN R, Generation R; UKB, UK Biobank.

for the superior and transverse temporal cortices (Braak stage V, figure 3B), we identified AD genetic liability to be associated with greater thickness ( $p$  for trend across age tertiles=0.03 and  $p=0.003$ , respectively).

We also identified effects which did not show clear age-dependent associations. Within the youngest UKB participants aged 45–60 years, a higher genetic liability to AD was associated with a greater thickness in the cuneus. In participants aged 60–68 years, a higher genetic liability to AD was associated with a lower volume in the caudate (Braak stage V, figure 3B), and putamen (Braak stage V, figure 3B). In participants aged 68–81 years, a doubling in odds of genetic liability to AD was associated with 0.05 SD (95% CI 0.07 to 0.02) lower thickness in the entorhinal cortex (Braak stage I), fusiform and parahippocampal cortices (Braak stage III, figure 3A). Additionally, AD genetic liability was associated with a thicker pericalcarine, postcentral, precentral cortex and a larger volume in the lateral ventricles (Braak stage VI, figure 3C).

Causal effects of brain morphology on risk of Alzheimer’s disease

We found little evidence of causal effects for the global measures of thickness and eTIV on AD risk (online supplemental table 11). However, of the eight subcortical structures examined, we observed that a 1 SD increase hippocampal volume, instrumented by six SNPs, increased AD risk on average by 33% (95% CI 1.11 to 1.59). A 1 SD increase in the thickness of the lateral orbitofrontal cortex increased AD risk (OR 2.74; 95% CI 1.08 to 6.93), while a 1 SD higher thickness in the rostral anterior cingulate cortex decreased AD risk (OR 0.40; 95% CI 0.19 to 0.83) (figure 4). However, for these two structures, we have one instrument and could not perform sensitivity analyses for assessing heterogeneity or pleiotropy.

Sensitivity analyses

Detailed results of analyses examining potential pleiotropy are provided in online supplemental tables 1–18. The evidence of a causal effect of genetic liability to AD on the caudal anterior cingulate in peri-pubertal childhood was consistent across pleiotropy-robust methods (SD  $-0.03$ ; 95% CI  $-0.06$  to  $-0.004$  in MR-Egger and SD  $-0.03$ ; 95% CI  $-0.05$  to  $-0.01$

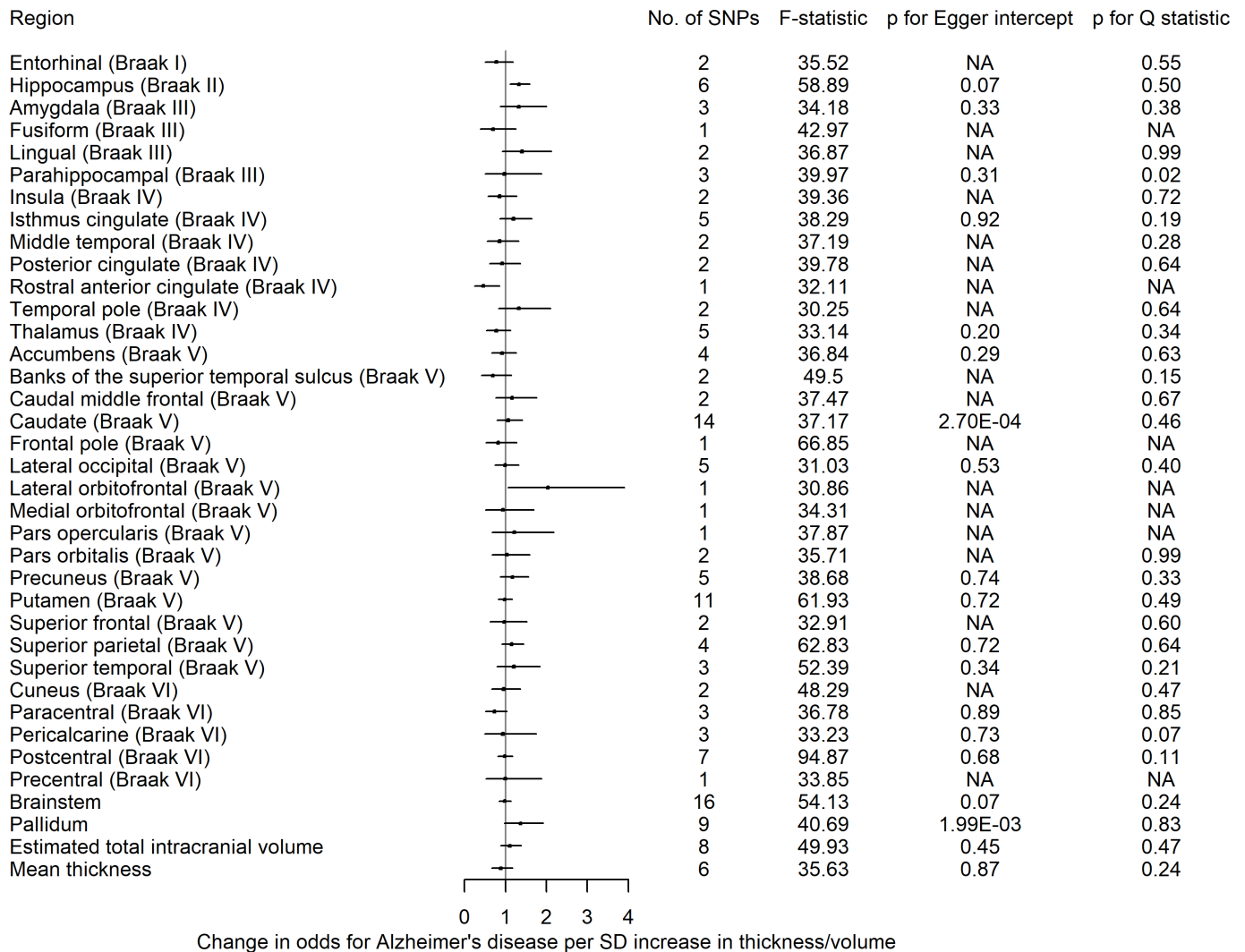


Figure 4 The causal effects of genetic predisposition to higher thickness and volume of cortical, subcortical and white matter measures, respectively on risk for AD. This figure shows the change in OR for AD per SD change in thickness and volume of cortical, subcortical structures, respectively. Effects for lateral ventricles is missing due to inability in obtaining access to summary statistics. The F-statistic is a measure of instrument strength. AD, Alzheimer’s disease; NA, not available.

per doubling in odds of genetic liability to AD for weighted mode). The association with thalamic volume in school-aged children and early adulthood were consistent across most of the pleiotropy-robust methods (online supplemental tables 4 and 8). In the analysis of AD genetic liability on brain structures in UKB, the magnitude of effect sizes for the MR-Egger, weighted median and mode were consistent with the IVW estimates for all brain structures (online supplemental table 9). In the MR analysis of brain structures on AD risk, the observed detrimental effect of a larger hippocampus on AD was consistent across pleiotropy-robust methods (online supplemental tables 11 and 18).

When we removed the *APOE* SNPs from our analyses in the peri-pubertal childhood cohort meta-analysis, the effect observed for AD liability on thalamic volume and the thickness of the caudal anterior cingulate cortex attenuated to the null (online supplemental table 19). The effect observed for AD liability on thalamic volume in early adulthood also attenuated to the null (online supplemental table 20). In UKB analyses, the associations with regional cortical thickness and subcortical structures largely remained (online supplemental table 21).

The directionality test indicated that, on average, the instruments for AD explained more variance in AD than they did in the brain structures in UKB (online supplemental table 22). The directionality test for SNPs associated with the hippocampus, lateral occipital and rostral anterior cingulate cortices on AD showed that they explain more variance in these structures than they do in AD risk (online supplemental table 23).

## DISCUSSION

Our findings suggest that AD risk alleles have an age-dependent effect on a range of cortical and subcortical brain measures across mid-to-late adulthood, but we found little evidence for such effects in childhood and early adulthood, with the exception of an observed effect of AD genetic liability on thalamic volume and the thickness of the caudal anterior cingulate. These results therefore suggest that genetic liability to AD operates largely through causing changes in brain morphology in later life (eg, potential neurodegeneration), rather than initial brain reserve. In the age-stratified analysis of UKB participants, a higher AD genetic liability was associated with an age-dependent decrease in the thickness of the middle temporal, inferior temporal cortices as well as volume of structures such as the hippocampus, accumbens and thalamus. Some effects were only apparent in the oldest participants (aged 68–81 years), such as the decrease in the thickness of the fusiform, entorhinal and parahippocampal cortices and the volume of the amygdala. When SNPs in the *APOE* gene region were removed, effects across all structures largely remained but as expected, became less precise. In the reverse direction, there was little evidence that the thickness and volume of cortical and subcortical structures, respectively, affected the risk of AD, except for a greater hippocampal volume increasing risk.

In adults, genetic liability to AD was associated with regions known to show significant atrophy early in disease progression, such as the entorhinal,<sup>47–49</sup> inferior, middle temporal and parahippocampal cortices,<sup>50</sup> as well as the hippocampus.<sup>51</sup> Change in hippocampal volume is an important imaging phenotype to define preclinical stages of AD, where atrophy predicts conversion from mild cognitive impairment to AD.<sup>52</sup> We observed a trend of a higher genetic liability to AD being associated with a smaller hippocampus in the younger participants, of ages 45–68 years. Additionally, there was strong evidence of an effect of genetic liability on a lower hippocampal volume in the oldest

age participants (aged 68–81 years), using genetic instruments both including and excluding the *APOE* locus. A study also using the UKB identified strong evidence of an effect of the AD PRS ( $p \leq 5 \times 10^{-8}$ ) and hippocampal subfield volumes in older individuals (aged 63–80 years), which was driven by SNPs in the *APOE* locus.<sup>51</sup> Contrary to previous PRS studies,<sup>12 13</sup> we found weak evidence that genetic liability to AD was associated with a lower hippocampal volume in childhood. However, in comparison with the stringent threshold we used in our study ( $p < 5 \times 10^{-8}$ ), these studies used liberal p-value thresholds for SNP inclusion ( $p \leq 0.132$  and  $p \leq 0.0001$ ) (increasing risk of bias due to horizontal pleiotropy).<sup>12 13</sup>

The focus of previous PRS studies with brain MRI data on the hippocampus and the neocortex can be attributed to their well-recognised role in cognition and episodic memory.<sup>53 54</sup> However, there are other structures that are relevant for cognition that are less well studied in relation to genetic liability to AD,<sup>55</sup> such as the thalamus. The medial temporal lobe connects to thalamic nuclei and the retrosplenial cortex, constituting the hippocampal-diencephalic system, whose integrity is important for normal episodic memory.<sup>56</sup> In our study, we found the earliest, most robust effects of genetic liability to AD in the thalamus as early as childhood (aged 8–14 years) and in the caudate and accumbens from 60 years of age. A study investigating how the *APOE* genotype changes whole-brain large-scale structural networks in subjects with mild cognitive impairment,<sup>57</sup> found *APOE*  $\epsilon 4$  carriers showed pronounced atrophy in specific regions such as the thalamus and the hippocampus, both of which had strong structural covariance association with the left caudate nucleus. Furthermore, a longitudinal brain imaging study examining the effects of the *APOE*  $\epsilon 4$  genotype found evidence of differences between carriers/non-carriers in rates of amyloid- $\beta$  plaque accumulation across the adult lifespan only in the caudate at age 56 years and the putamen at age 63 years.<sup>58</sup> *APOE*  $\epsilon 4$  carriers showed accelerated rates of amyloid-beta deposition in the entorhinal cortex at age 68 years. We observed that the oldest participants (aged 68–81 years) with higher genetic liability to AD showed, on average, lower entorhinal thickness.

Like other studies, we also found causal effects of genetic liability to AD on larger thickness in the lateral occipital, which is consistent with two previous studies in healthy individuals where *APOE*  $\epsilon 4$  carriers have a thicker occipital cortex in comparison with normal controls.<sup>59 60</sup> The thickening of certain brain regions has been speculated to reflect brain swelling in response to glial activation in preclinical AD stages.<sup>61</sup>

Genetic liability to AD is hypothesised to affect brain structures through influencing neurodevelopment, resulting in structural differences in the brain which may increase tolerance to pathology (ie, altering brain reserve and increasing the age of disease onset), or by changing the rates or mechanisms of neurodegeneration.<sup>3</sup> We observe an age-dependent decrease in the volume of structures such as the thalamus, caudate and accumbens in UKB participants. However, a longitudinal analysis would be required to test the variable neurodegeneration hypothesis and such a conclusion cannot be extrapolated from findings in cross-sectional data (as in our analyses). Walhovd *et al* examined the association between AD PRS and hippocampal volume in 1181 cognitively healthy people with a wide age range (4–95 years).<sup>4</sup> They identified an effect of a higher AD PRS on reduced hippocampal volumes in young adults, which was consistent across age groups, suggesting the AD PRS results in an earlier onset of brain ageing instead of accelerated ageing through variable neurodegeneration. The MR of brain morphology on AD in our study provides little support for the notion that

brain structure alterations change the risk for AD, except for a larger hippocampal volume increasing the risk for AD, which is contrary to most existing research.<sup>4 62 63</sup> This hippocampus finding from our MR study may be due to chance, or due to the small number of SNPs used (n=6). It is unlikely that these effects are a result of pathways independent of hippocampal volume (ie, horizontal pleiotropy), as the MR estimators which relax the assumptions about instrument validity are consistent with the IVW method, and there was little evidence of heterogeneity or pleiotropy in the causal effect estimates. Although we found little evidence of effects of brain morphology on AD risk, we observed that AD genetic liability influenced the volume of the thalamus from childhood to adulthood, which suggests that initial thalamic reserve could potentially play a role in AD risk. However, given that this structure is not typically implicated in the earliest AD-related brain atrophy, it is possible that this is a chance finding reflecting variability around the null. The caudal anterior cingulate was observed to be associated with genetic effects in childhood but not in adulthood. However, a recent recall-by-genotype study also reported an effect in this region in adults of the PROTECT cohort.<sup>64</sup> In summary, the fewer effects observed in childhood and early adulthood compared with those later in the life course may be due to developmental noise, or a greater effect of genetic variation on more biological pathways in older individuals. It is also possible that genetic effects become more pronounced later in the life course due to the accumulation of gene-environment interactions and/or potential epigenetic mechanisms. Future studies should seek to replicate this in large independent samples with repeated measures when more data become available.

The MR method requires that genetic variants must fulfil three key assumptions to be considered valid instrumental variables: (1) that the genetic variants are strongly associated with the exposure (relevance assumption), (2) that there is no confounding of the genetic instrument – outcome association (eg, by population stratification, or dynastic effects; the independence assumption), and (3) that the genetic instruments affect the outcome only through the exposure (exclusion restriction assumption). Only the first assumption can be tested with the use of statistical parameters indicating instrument strength (variants associated with the trait at genome-wide significance and/or F-statistics in our analyses >10). The independence and exclusion restriction assumptions are not testable but are falsifiable with sensitivity analyses. We adjusted our GWAS for ancestry-informative principal components to control for population stratification. We were unable to account for dynastic effects in this study, but future within-family MR study designs should look to examine this. For the exclusion-restriction assumption, sensitivity analyses were performed to examine potential bias due to horizontal pleiotropy. That said, several brain measures had too few genetic proxies for pleiotropy sensitivity analyses to be performed and hence, these results should be considered with caution.

While previous studies have examined whether genetic liability to AD is associated with specific structural brain measures, our study is the first to examine these in such large samples, using an exploratory approach from childhood to old age. One of the main strengths of our study is that genetic variants are subject to little measurement error, contrary to observational neuroimaging phenotypes, and can serve as unconfounded indicators of particular traits values.<sup>17</sup> Furthermore, using aggregate PRS precludes the examination of key potential sources of bias such as horizontal pleiotropy, which we have examined in detail here. We examined regions that have not been shown to be vulnerable

to AD pathology, allowing us to discover novel regions affected by genetic liability to AD, such as the caudate. The large modern biobanks with neuroimaging and genetic data allowed us to recreate to the best of our ability a pseudo-longitudinal cohort. The precision of age-dependent dose effects suggest that our results are unlikely to be due to chance or other forms of bias. However, for studies such as ALSPAC, participants were selected for imaging for (1) a case-control study of psychotic experiences, (2) recall-by-genotype for schizophrenia, (3) testosterone study, making the ALSPAC sample unrepresentative of the general population. Another limitation is that different Free-surfer versions were used across cohorts. However, we allowed for this technical variation using random-effects meta-analyses. Although we applied multiple correction strategies controlling the false discovery rate, our findings were consistent across multiple cohorts. Finally, the participants in our analyses were of European ancestry and the findings may not be generalisable to other populations.

Our study shows that genetic liability to AD is associated with age-dependent changes in brain morphology in non-clinical populations, starting as early as 60 years of age, potentially highlighting the earliest phenotypic manifestations of the disease and the optimal timing for intervention with any potential neuroprotective therapy. Brain imaging to detect AD focuses on hippocampal, whole brain and parietal volume. The findings of our study highlight the importance of brain volume in other regions — notably the striatum — for AD. The analysis of these regions could be incorporated into early diagnosis imaging analysis algorithms for clinical use. The lack of evidence to support an effect of brain morphology on AD suggests that genetic liability to AD affects biological pathways leading to neurodegeneration rather than neurodevelopment. Future research should aim to use a longitudinal design and integrate their findings with biological and clinical data.

#### Author affiliations

<sup>1</sup>Medical Research Council Integrative Epidemiology Unit, University of Bristol, Bristol, UK

<sup>2</sup>Population Health Sciences, University of Bristol, Bristol, UK

<sup>3</sup>The Generation R Study Group, Erasmus MC University Medical Center, Rotterdam, UK

<sup>4</sup>Department of Child and Adolescent Psychiatry and Psychology, Erasmus MC University Medical Center, Rotterdam, The Netherlands

<sup>5</sup>Bristol Medical School, University of Bristol, Bristol, UK

<sup>6</sup>North Bristol NHS Trust, Bristol, UK

<sup>7</sup>Department of Psychology, University of Bath, Bath, UK

<sup>8</sup>Department of Radiology and Nuclear Medicine, Erasmus University School of Medicine, Rotterdam, UK

<sup>9</sup>Department of Epidemiology, Erasmus MC University Medical Center Rotterdam, Rotterdam, The Netherlands

<sup>10</sup>Biostatistics and Health Informatics Department, King's College London, Boston, UK

<sup>11</sup>Department of Social and Behavioral Sciences, Harvard T H Chan School of Public Health, Boston, Massachusetts, USA

<sup>12</sup>Department of Child and Adolescent Psychiatry and Psychotherapy, Heidelberg University, Heidelberg, Germany

<sup>13</sup>Psychiatry, Trinity College Dublin, Dublin, Ireland

<sup>14</sup>Kings College London, Centre for Population Neuroscience and Precision Medicine (PONS), London, UK

<sup>15</sup>Institute of Cognitive and Clinical Neuroscience, Central Institute of Mental Health, University of Mannheim, Mannheim, Germany

<sup>16</sup>Psychology, School of Social Sciences, University of Mannheim, Mannheim, Germany

<sup>17</sup>Neurospin, LNAO, I2BM, CEA, Saclay, France

<sup>18</sup>University of Vermont, Burlington, Vermont, USA

<sup>19</sup>University of Nottingham, Nottingham, UK

<sup>20</sup>Department of Psychiatry and Psychotherapy CCM, Berlin Institute of Health, Berlin, Germany

<sup>21</sup>Physikalisch-Technische Bundesanstalt (PTB), Braunschweig, Germany



- <sup>22</sup>Institut National de la Santé et de la Recherche Médicale, INSERM U1299, Paris, France
- <sup>23</sup>Centre Borelli, Cachan, France
- <sup>24</sup>Institute of Medical Psychology and Medical Sociology, Kiel University, Kiel, Germany
- <sup>25</sup>NeuroSpin, Université Paris-Saclay, Gif-sur-Yvette, France
- <sup>26</sup>Departments of Psychology and Psychiatry, University of Toronto, Toronto, Ontario, Canada
- <sup>27</sup>Department of Psychiatry, University of Montreal, Montreal, Quebec, Canada
- <sup>28</sup>Department of Child and Adolescent Psychiatry and Psychotherapy, University Medical Centre Göttingen, Göttingen, Germany
- <sup>29</sup>Department of Psychiatry, Technische Universität Dresden, Dresden, Germany
- <sup>30</sup>Department of Psychiatry and Psychotherapy CCM, Charité Universitätsmedizin Berlin, Berlin, Germany
- <sup>31</sup>Berlin Institute of Health at Charite, Berlin, Germany
- <sup>32</sup>Department of Education and Psychology, Freie Universität Berlin, Berlin, Germany
- <sup>33</sup>Trinity Centre for Bioengineering, Trinity College Dublin, Dublin, Ireland
- <sup>34</sup>Fudan University, Shanghai, People's Republic of China
- <sup>35</sup>PONS Centre, Dept. of Psychiatry and Clinical Neuroscience, CCM, Berlin, Germany
- <sup>36</sup>University College London Division of Psychiatry, London, UK

X Elizabeth Coulthard @lizcoulthard and Alfie Wearn @AlfieWearn

**Acknowledgements** Data used in the preparation of this article were obtained from the Adolescent Brain Cognitive Development (ABCD) Study (<https://abcdstudy.org>), held in the NIMH Data Archive (NDA). This is a multisite, longitudinal study designed to recruit >10 000 children aged 9–10 years and follow them over 10 years into early adulthood. The ABCD study is supported by the National Institutes of Health (NIH) and additional federal partners under award numbers U01DA041048, U01DA050989, U01DA051016, U01DA041022, U01DA051018, U01DA051037, U01DA050987, U01DA041174, U01DA041106, U01DA041117, U01DA041028, U01DA041134, U01DA050988, U01DA051039, U01DA041156, U01DA041025, U01DA041120, U01DA051038, U01DA041148, U01DA041093, U01DA041089, U24DA041123, U24DA041147. A full list of supporters is available at <https://abcdstudy.org/federal-partners.html>. A listing of participating sites and a complete listing of the study investigators can be found at [https://abcdstudy.org/consortium\\_members/](https://abcdstudy.org/consortium_members/). ABCD consortium investigators designed and implemented the study and/or provided data but did not necessarily participate in analysis or writing of this report. The ABCD data repository grows and changes over time. The ABCD data used in this report came from NIMH Data Archive Digital Object Identifier (10.15154/1503209). We are extremely grateful to all the families who took part in this study, the midwives for their help in recruiting them and the whole ALSPAC team, which includes interviewers, computer and laboratory technicians, clerical workers, research scientists, volunteers, managers, receptionists and nurses. The UK Medical Research Council and Wellcome (grant ref: 217065/Z/19/Z) and the University of Bristol provide core support for ALSPAC. This publication is the work of RK-L and ELA and NMD will serve as guarantors for the contents of this paper. A comprehensive list of grants funding is available on the ALSPAC website (<http://www.bristol.ac.uk/alspac/external/documents/grant-acknowledgements.pdf>). The ALSPAC-Testosterone study was funded by the NIH, USA (R01MH085772 to TP). The ALSPAC-PE study was funded by a grant from the UK Medical Research Council (G0901885). ASD was also supported by the NIH Research Biomedical Research Centre at the South London and Maudsley Hospital Foundation NHS Trust and the IoPPN, King's College London. The ALSPAC SCZ-RbG study was funded by grant MR/K004360/1 from the Medical Research Council (MRC) titled: 'Behavioural and neurophysiological effects of schizophrenia risk genes: a multi-locus, pathway based approach' and by the MRC Centre for Neuropsychiatric Genetics and Genomics (G0800509) and the NIHR Bristol Biomedical Research Centre. IMAGEN is supported by the European Union-funded FP6 Integrated Project IMAGEN (reinforcement-related behaviour in normal brain function and psychopathology) (LSHM-CT-2007-037286), the Horizon 2020 funded ERC Advanced Grant 'STRATIFY' (brain network-based stratification of reinforcement-related disorders) (695313), Human Brain Project (HBP SGA 2, 785907 and HBP SGA 3, 945539), the Medical Research Council Grant 'c-VEDA' (Consortium on Vulnerability to Externalising Disorders and Addictions) (MR/N000390/1), the National Institute of Health (NIH) (R01DA049238, a decentralised macro and micro gene-by-environment interaction analysis of substance use behaviour and its brain biomarkers), the National Institute for Health Research (NIHR) Biomedical Research Centre at South London and Maudsley NHS Foundation Trust and King's College London, the Bundesministerium für Bildung und Forschung (BMBF grants 01GS08152; 01EV0711; Forschungsnetz AERIAL 01EE1406A, 01EE1406B; Forschungsnetz IMAC-Mind 01GL1745B), the Deutsche Forschungsgemeinschaft (DFG grants SM 80/7-2, SFB 940, TRR 265, NE 1383/14-1), the Medical Research Foundation and Medical Research Council (grants MR/R00465X/1 and MR/S020306/1), the NIH funded ENIGMA (grants 5U54EB020403-05 and 1R56AG058854-01). Further support was provided by grants from the ANR (ANR-12-SAMA-0004, AAPG2019 — GeBra), the Eranet Neuron (AF12-NEUR0008-01 — WM2NA and ANR-18-NEUR00002-01 — ADORé), the Fondation de France (00081242), the Fondation pour la Recherche Médicale

(DPA20140629802), the Mission Interministérielle de Lutte-contre-les-Drogues-et-les-Conduites-Addictives (MILDECA), the Assistance-Publique-Hôpitaux-de-Paris and INSERM (interface grant), Paris Sud University IDEX 2012, the Fondation de l'Avenir (grant AP-RM-17-013), the Fédération pour la Recherche sur le Cerveau; the NIH, Science Foundation Ireland (16/ERC/D/3797), USA (Axon, Testosterone and Mental Health during Adolescence; RO1 MH085772-01A1) and by NIH Consortium grant U54 EB020403, supported by a cross-NIH alliance that funds Big Data to Knowledge Centres of Excellence. The UK Biobank data used in this work were obtained from UK Biobank Data Application 48970. We thank UK Biobank for making the data available, and to all UK Biobank study participants, who generously donated their time to make this resource possible. We thank the International Genomics of Alzheimer's Project (IGAP) for providing summary results data for these analyses. The investigators within IGAP contributed to the design and implementation of IGAP and/or provided data but did not participate in analysis or writing of this report. IGAP was made possible by the generous participation of the control subjects, the patients and their families. The i-Select chips was funded by the French National Foundation on Alzheimer's disease and related disorders. EADI was supported by the LABEX (laboratory of excellence programme investment for the future) DISTALZ grant, INSERM, Institut Pasteur de Lille, Université de Lille 2 and the Lille University Hospital. GERAD/PERADES was supported by the Medical Research Council (grant no. 503480), Alzheimer's Research UK (grant no. 503176), the Wellcome Trust (grant no. 082604/2/07/Z) and German Federal Ministry of Education and Research (BMBF): Competence Network Dementia (CND) grant no. 01GI0102, 01GI0711, 01GI0420. CHARGE was partly supported by the NIH/NIA grant R01 AG033193 and the NIA AG081220 and AGES contract N01-AG-12100, the NHLBI grant R01 HL105756, the Icelandic Heart Association and the Erasmus Medical Center and Erasmus University. ADGC was supported by the NIH/NIA grants U01 AG032984, U24 AG021886, U01 AG016976, and the Alzheimer's Association grant ADGC-10-196728.

**Contributors** RK-L, ELA, NMD, LDH and YB-S designed, conceptualised and interpreted results of the study. RK-L and BX performed the statistical analyses. EC, EW, TS, TW and AW provided advice regarding structural brain measures. GH provided advice and feedback on the implementation of software. TS, AB, SD, HF, AG, HG, PG, AH, RB, J-LM, M-LPM, EA, FN, DPO, TP, LP, SM, JHF, MS, HW, RW, GS, and JW worked on the processing and provision of IMAGEN data. All authors provided valuable feedback and comments on the manuscript. ELA and NMD will serve as guarantors for the contents of this paper.

**Funding** RK-L was supported by a Wellcome Trust PhD studentship (grant ref: 215193/Z/18/Z). ELA is supported by a fellowship from the UK Medical Research Council (MR/P014437/1). The Medical Research Council (MRC) and the University of Bristol support the MRC Integrative Epidemiology Unit (MC\_UU\_00011/1). NMD is supported by a Norwegian Research Council Grant number 295989. YB-S receives grant funding from the following: MRC, Wellcome Trust, NIHR, Templeton Foundation, Parkinson's UK, HQIP, Versus Arthritis, Dunhill Medical Trust, Gatsby Foundation, Kidney Research UK. LDH is funded by a Career Development Award from the UK Medical Research Council (MR/M020894/1). EW is funded by the European Union's Horizon 2020 research and innovation programme (grant no. 848158) and by CLOSER, who was funded by the Economic and Social Research Council (ESRC) and the MRC between 2012 and 2017. Its initial 5-year grant has since been extended to March 2021 by the ESRC (grant reference: ES/K000357/1). TW is funded by Netherlands Organization for Health Research and Development (ZonMw) TOP project number 91211021. This research was also supported by contract R01-HL105756-07 from the National Heart, Lung and Blood Institute (NHLBI). EC is supported by grants with the Above and Beyond Charity for research optimising sleep to slow dementia progression and improve quality of life and the Alzheimer's Research UK on research about the long-term memory testing to predict the presence of Alzheimer's disease pathology from BRACE charity. CC is supported by the European Union's Horizon 2020 Research and Innovation Programme under the Marie Skłodowska-Curie grant agreement no. 707404 and grant agreement no. 848158 (EarlyCause Project). The work of Henning Tiemeier is supported by Netherlands Organization for Health Research and Development (ZonMw: 016.VICI.170.200). GH is supported by the Wellcome Trust and Royal Society (208806/Z/17/Z). AW is supported by Wellcome Trust PhD Grant, BRACE Pilot grant (co-applicant). SD is supported by the MRC. AB has received two grants from the National Children's Hospital Foundation — Tallaght (Ireland), a grant from the Health Research Board (Ireland), a grant from the Irish Research Council and a grant from the European Union Horizon 2020 Programme (MSCA-ITN). All funds paid to Trinity College Dublin. HF is supported by the Covidrug German Research Foundation Perpain German Ministry of Education and Research. TP is supported by the Canadian Institutes of Health research. MS is supported by the Deutsche Forschungsgemeinschaft, grant numbers 186318919, 178833530 and 402170461. HW is supported by EU Horizon 2020: GA101016127; GA 777084, European Research Commission: GA 695313, BMBF (German Ministry for Health and Education): 01ZX1909C, 01EE1407G, 01ZX1614B, DFG (German Research Foundation): SFB 940; TRR 256/1; GRK 2386; WA 1539/9-1; WA 1539/11-1.

**Disclaimer** This manuscript reflects the views of the authors and may not reflect the opinions or views of the NIH or ABCD consortium investigators.

**Competing interests** TB served in an advisory or consultancy role for Lundbeck, Medice, Neurim Pharmaceuticals, Oberberg GmbH, Shire. He received conference support or speaker's fee by Lilly, Medice, Novartis and Shire. He has been involved in clinical trials conducted by Shire & Viforpharma. He received royalties from Hogrefe, Kohlhammer, CIP Medien, Oxford University Press. The present work is unrelated to the above grants and relationships. LP served in an advisory or consultancy role for Roche and Viforpharm and received speaker's fee by Shire. She received royalties from Hogrefe, Kohlhammer and Schattauer. The present work is unrelated to the above grants and relationships.

**Patient consent for publication** Not applicable.

**Ethics approval** UK Biobank is approved by the National Health Service National Research Ethics Service (ref 11/NW/0382; UK Biobank application number 48970). Ethics approval for the study was obtained from the ALSPAC Ethics and Law Committee and the Local Research Ethics Committees and informed consent for the use of data collected via questionnaires and clinics was obtained from participants. In Generation R, all study protocols and measurements assessed in each wave of data collection were approved by the Medical Ethical Committee (MEC 198.782/2001/31) of the Erasmus MC, University Medical Center Rotterdam. The IMAGEN study was approved by the institutional ethics committee of Kings College London, University of Nottingham, Trinity College Dublin, University of Heidelberg, Technische Universität Dresden, Commissariat à l'Énergie Atomique et aux Énergies Alternatives and University Medical Center at the University of Hamburg in accordance with the Declaration of Helsinki. The UCSD IRB approved all data collection protocols for ABCD. IRB number: 160091. All analyses in this study used de-identified data, therefore no additional IRB approval was required. Participants gave informed consent to participate in the study before taking part.

**Provenance and peer review** Not commissioned; externally peer reviewed.

**Data availability statement** Data may be obtained from a third party and are not publicly available. The ENIGMA consortium MRI summary measures from genetic association analyses of estimated total intracranial volume, subcortical structures as well as cortical thickness were requested online. The ABCD study data are openly available to qualified researchers for free (<https://nda.nih.gov/abcd/request-access>). Requests for Generation R data should be directed towards the management team of the Generation R study ([secretariaat.gen@erasmusmc.nl](mailto:secretariaat.gen@erasmusmc.nl)), which has a protocol of approving data requests. For access to IMAGEN data, researchers may submit a request to the IMAGEN consortium (<https://imagen-europe.com/resources/imagen-project-proposal/>). ALSPAC details and data descriptions are available on their website ([www.bristol.ac.uk/alspac/researchers/access](http://www.bristol.ac.uk/alspac/researchers/access)), where applications for individual-level data can be made (managed access). UK Biobank data are available through a procedure described on their website (<http://www.ukbiobank.ac.uk/using-the-resource/>). The UCSD IRB approved all data collection protocols for ABCD. IRB number: 160091. In Generation R, all study protocols and measurements assessed in each wave of data collection were approved by the Medical Ethical Committee (MEC 198.782/2001/31) of the Erasmus MC, University Medical Center Rotterdam. The IMAGEN study was approved by the institutional ethics committee of Kings College London, University of Nottingham, Trinity College Dublin, University of Heidelberg, Technische Universität Dresden, Commissariat à l'Énergie Atomique et aux Énergies Alternatives, and University Medical Center at the University of Hamburg in accordance with the Declaration of Helsinki. Ethics approval for the study was obtained from the ALSPAC Ethics and Law Committee and the Local Research Ethics Committees and informed consent for the use of data collected via questionnaires and clinics was obtained from participants. UK Biobank is approved by the National Health Service National Research Ethics Service (ref 11/NW/0382; UK Biobank application number 48970). All analyses in this study used de-identified data, therefore no additional IRB approval was required. All necessary patient/participant consent has been obtained. Code is available at [https://github.com/rsk192/AD\\_BRAIN\\_BIDIRECTIONAL\\_MR](https://github.com/rsk192/AD_BRAIN_BIDIRECTIONAL_MR).

**Supplemental material** This content has been supplied by the author(s). It has not been vetted by BMJ Publishing Group Limited (BMJ) and may not have been peer-reviewed. Any opinions or recommendations discussed are solely those of the author(s) and are not endorsed by BMJ. BMJ disclaims all liability and responsibility arising from any reliance placed on the content. Where the content includes any translated material, BMJ does not warrant the accuracy and reliability of the translations (including but not limited to local regulations, clinical guidelines, terminology, drug names and drug dosages), and is not responsible for any error and/or omissions arising from translation and adaptation or otherwise.

**Open access** This is an open access article distributed in accordance with the Creative Commons Attribution 4.0 Unported (CC BY 4.0) license, which permits others to copy, redistribute, remix, transform and build upon this work for any purpose, provided the original work is properly cited, a link to the licence is given, and indication of whether changes were made. See: <https://creativecommons.org/licenses/by/4.0/>.

#### ORCID iDs

Roxanna Korologou-Linden <http://orcid.org/0000-0002-9887-4763>

Elizabeth Coulthard <http://orcid.org/0000-0002-0017-9595>

Alfie Wearn <http://orcid.org/0000-0001-7699-648X>

Arun Bokde <http://orcid.org/0000-0003-0114-4914>

Emma Louise Anderson <http://orcid.org/0000-0002-1508-0598>

#### REFERENCES

- Yang J, Pan P, Song W, *et al.* Voxelwise meta-analysis of gray matter anomalies in Alzheimer's disease and mild cognitive impairment using anatomic likelihood estimation. *J Neurol Sci* 2012;316:21–9.
- Bateman RJ, Xiong C, Benzinger TLS, *et al.* Clinical and biomarker changes in dominantly inherited Alzheimer's disease. *N Engl J Med* 2012;367:795–804.
- Stern Y. Cognitive reserve in ageing and Alzheimer's disease. *Lancet Neurol* 2012;11:1006–12.
- Walhovd KB, Fjell AM, Sørensen Ø, *et al.* Genetic risk for Alzheimer disease predicts hippocampal volume through the human lifespan. *Neurol Genet* 2020;6:e506.
- Mormino EC, Sperling RA, Holmes AJ, *et al.* Polygenic risk of Alzheimer disease is associated with early- and late-life processes. *Neurology* 2016;87:481–8.
- Sabuncu MR, Buckner RL, Smoller JW, *et al.* The association between a polygenic Alzheimer score and cortical thickness in clinically normal subjects. *Cereb Cortex* 2012;22:2653–61.
- Grasby KL, Jahanshad N, Painter JN, *et al.* The genetic architecture of the human cerebral cortex. *Science* 2020;367:eaay6690.
- Jansen IE, Savage JE, Watanabe K, *et al.* Genome-wide meta-analysis identifies new loci and functional pathways influencing Alzheimer's disease risk. *Nat Genet* 2019;51:404–13.
- Kunkle BW, Grenier-Boley B, Sims R, *et al.* Genetic meta-analysis of diagnosed Alzheimer's disease identifies new risk loci and implicates Aβ, Tau, immunity and lipid processing. *Nat Genet* 2019;51:414–30.
- Lambert JC, Ibrahim-Verbaas CA, Harold D, *et al.* Meta-analysis of 74,046 individuals identifies 11 new susceptibility loci for Alzheimer's disease. *Nat Genet* 2013;45:1452–8.
- Corder EH, Saunders AM, Strittmatter WJ, *et al.* Gene dose of apolipoprotein E type 4 allele and the risk of Alzheimer's disease in late onset families. *Science* 1993;261:921–3.
- Axelrud LK, Santoro ML, Pine DS, *et al.* Polygenic risk score for Alzheimer's disease: implications for memory performance and hippocampal volumes in early life. *Am J Psychiatry* 2018;175:555–63.
- Foley SF, Tansey KE, Caseras X, *et al.* Multimodal brain imaging reveals structural differences in Alzheimer's disease polygenic risk carriers: a study in healthy young adults. *Biol Psychiatry* 2017;81:154–61.
- Satizabal CL, Adams HHH, Hibar DP, *et al.* Genetic architecture of subcortical brain structures in 38,851 individuals. *Nat Genet* 2019;51:1624–36.
- Hibar DP, Stein JL, Renteria ME, *et al.* Common genetic variants influence human subcortical brain structures. *Nature* 2015;520:224–9.
- Elliott LT, Sharp K, Alfaro-Almagro F, *et al.* Genome-wide association studies of brain imaging phenotypes in UK biobank. *Nature* 2018;562:210–6.
- Davey Smith G, Hemani G. Mendelian randomization: genetic anchors for causal inference in epidemiological studies. *Human Molecular Genetics* 2014;23:R89–98.
- Desikan RS, Cabral HJ, Hess CP, *et al.* Automated MRI measures identify individuals with mild cognitive impairment and Alzheimer's disease. *Brain* 2009;132:2048–57.
- Adams HHH, Hibar DP, Chouraki V, *et al.* Novel genetic loci underlying human intracranial volume identified through genome-wide association. *Nat Neurosci* 2016;19:1569–82.
- Hibar DP, Adams HHH, Jahanshad N, *et al.* Novel genetic Loci associated with hippocampal volume. *Nat Commun* 2017;8:13624.
- White T, El Marroun H, Nijs I, *et al.* Pediatric population-based neuroimaging and the generation R study: the intersection of developmental neuroscience and epidemiology. *Eur J Epidemiol* 2013;28:99–111.
- Muetzel RL, Mulder RH, Lamballais S, *et al.* Frequent bullying involvement and brain morphology in children. *Front Psychiatry* 2019;10:696.
- Casey BJ, Cannonier T, Conley MI, *et al.* The Adolescent Brain Cognitive Development (ABCD) study: imaging acquisition across 21 sites. *Dev Cogn Neurosci* 2018;32:43–54.
- Hagler DJ, Hatton S, Cornejo MD, *et al.* Image processing and analysis methods for the adolescent brain cognitive development study. *Neuroimage* 2019;202.
- Schumann G, Loth E, Banaschewski T, *et al.* The IMAGEN study: reinforcement-related behaviour in normal brain function and psychopathology. *Mol Psychiatry* 2010;15:1128–39.
- Boyd A, Golding J, Macleod J, *et al.* Cohort profile: the 'children of the 90s'-The index offspring of the avon longitudinal study of parents and children. *Int J Epidemiol* 2013;42:111–27.
- Fraser A, Macdonald-Wallis C, Tilling K, *et al.* Cohort profile: the avon longitudinal study of parents and children: ALSPAC mothers cohort. *Int J Epidemiol* 2013;42:97–110.
- Northstone K, Lewcock M, Groom A, *et al.* The Avon longitudinal study of parents and children (ALSPAC): an update on the enrolled sample of index children in 2019 [version 1; peer review: 2 approved]. *Wellcome Open Res* 2019;4:51.

- 29 Miller KL, Alfaro-Almagro F, Bangarter NK, *et al.* Multimodal population brain imaging in the UK biobank prospective epidemiological study. *Nat Neurosci* 2016;19:1523–36.
- 30 Lawlor DA. Commentary: two-sample mendelian randomization: opportunities and challenges. *Int J Epidemiol* 2016;45:908–15.
- 31 Desikan RS, Ségonne F, Fischl B, *et al.* An automated labeling system for subdividing the human cerebral cortex on MRI scans into gyral based regions of interest. *Neuroimage* 2006;31:968–80.
- 32 Burgess S, Thompson SG, CRP CHD Genetics Collaboration. Avoiding bias from weak instruments in mendelian randomization studies. *Int J Epidemiol* 2011;40:755–64.
- 33 Burgess S, Labrecque JA. Mendelian randomization with a binary exposure variable: interpretation and presentation of causal estimates. *Eur J Epidemiol* 2018;33:947–52.
- 34 Schwarzer G. Meta: an R package for meta-analysis. *R News* 2015;7:40–5.
- 35 Stata press, STATA statistical software: release 16. [Preprint]; 2019.
- 36 Sadreev II, Elsworth BL, Mitchell RE, *et al.* Navigating sample overlap, winner's curse and weak instrument bias in mendelian randomization studies using the UK biobank. *medRxiv* [Preprint] 2021.
- 37 Bowden J, Davey Smith G, Burgess S. Mendelian randomization with invalid instruments: effect estimation and bias detection through egger regression. *Int J Epidemiol* 2015;44:512–25.
- 38 Egger M, Davey Smith G, Schneider M, *et al.* Bias in meta-analysis detected by a simple, graphical test. *BMJ* 1997;315:629–34.
- 39 Bowden J, Davey Smith G, Haycock PC, *et al.* Consistent estimation in mendelian randomization with some invalid instruments using a weighted median estimator. *Genet Epidemiol* 2016;40:304–14.
- 40 Hartwig FP, Davey Smith G, Bowden J. Robust inference in summary data Mendelian randomization via the zero modal pleiotropy assumption. *Int J Epidemiol* 2017;46:1985–98.
- 41 Hemani G, Tilling K, Davey Smith G. Orienting the causal relationship between imprecisely measured traits using GWAS summary data. *PLoS Genet* 2017;13:e1007081.
- 42 Wasserstein RL, Lazar NA. The ASA statement on p-Values: context, process, and purpose. *Am Stat* 2016;70:129–33.
- 43 Sterne JA, Davey Smith G. Sifting the evidence—what's wrong with significance tests? *BMJ* 2001;322:226–31.
- 44 White T, Muetzel RL, El Marroun H, *et al.* Paediatric population neuroimaging and the generation R study: the second wave. *Eur J Epidemiol* 2018;33:99–125.
- 45 White T, Jansen PR, Muetzel RL, *et al.* Automated quality assessment of structural magnetic resonance images in children: comparison with visual inspection and surface-based reconstruction. *Hum Brain Mapp* 2018;39:1218–31.
- 46 Sharp TH, McBride NS, Howell AE, *et al.* Population neuroimaging: generation of a comprehensive data resource within the ALSPAC pregnancy and birth cohort. *Wellcome Open Res* 2020;5:203.
- 47 Desikan RS, Schork AJ, Wang Y, *et al.* Polygenic overlap between C-reactive protein, plasma lipids, and alzheimer disease. *Circulation* 2015;131:2061–9.
- 48 Killiany RJ, Hyman BT, Gomez-Isla T, *et al.* MRI measures of entorhinal cortex vs hippocampus in preclinical AD. *Neurology* 2002;58:1188–96.
- 49 Tan CH, Bonham LW, Fan CC, *et al.* Polygenic hazard score, amyloid deposition and alzheimer's neurodegeneration. *Brain* 2019;142:460–70.
- 50 Köhler S, Black SE, Sinden M, *et al.* Memory impairments associated with hippocampal versus parahippocampal-gyrus atrophy: an MR volumetry study in Alzheimer's disease. *Neuropsychologia* 1998;36:901–14.
- 51 Foo H, Thalamuthu A, Jiang J, *et al.* Associations between Alzheimer's disease polygenic risk scores and hippocampal subfieldvolumes in 17,161 UK biobank participants. *Neurobiol Aging* 2021;98:108–15.
- 52 Macdonald KE, Bartlett JW, Leung KK, *et al.* The value of hippocampal and temporal horn volumes and rates of change in predicting future conversion to ad. *Alzheimer Dis Assoc Disord* 2013;27:168–73.
- 53 Squire LR, Stark CEL, Clark RE. The medial temporal lobe. *Annu Rev Neurosci* 2004;27:279–306.
- 54 Diana RA, Yonelinas AP, Ranganath C. Imaging recollection and familiarity in the medial temporal lobe: a three-component model. *Trends Cogn Sci* 2007;11:379–86.
- 55 Aggleton JP, Pralus A, Nelson AJD, *et al.* Thalamic pathology and memory loss in early Alzheimer's disease: moving the focus from the medial temporal lobe to papez circuit. *Brain* 2016;139:1877–90.
- 56 Opitz B, Friederici AD. Interactions of the hippocampal system and the Prefrontal cortex in learning language-like rules. *Neuroimage* 2003;19:1730–7.
- 57 Novellino F, López ME, Vaccaro MG, *et al.* Association between hippocampus, thalamus, and caudate in mild cognitive impairment APOEε4 carriers: a structural covariance MRI study. *Front Neurol* 2019;10:1303.
- 58 Mishra S, Blazey TM, Holtzman DM, *et al.* Longitudinal brain imaging in preclinical alzheimer disease: impact of APOE E4 genotype. *Brain* 2018;141:1828–39.
- 59 Espeseth T, Westlye LT, Fjell AM, *et al.* Accelerated age-related cortical thinning in healthy carriers of apolipoprotein E E4. *Neurobiol Aging* 2008;29:329–40.
- 60 Espeseth T, Westlye LT, Walhovd KB, *et al.* Apolipoprotein E E4-related thickening of the cerebral cortex modulates selective attention. *Neurobiol Aging* 2012;33:304–322.
- 61 Calsolaro V, Edison P. Neuroinflammation in Alzheimer's disease: current evidence and future directions. *Alzheimers Dement* 2016;12:719–32.
- 62 Stern Y, Barnes CA, Grady C, *et al.* Brain reserve, cognitive reserve, compensation, and maintenance: operationalization, validity, and mechanisms of cognitive resilience HHS public access. *Neurobiol Aging* 2019;83:124–9.
- 63 Bonner-Jackson A, Mahmoud S, Miller J, *et al.* Verbal and non-verbal memory and hippocampal volumes in a memory clinic population. *Alzheimers Res Ther* 2015;7:61.
- 64 Lancaster T, Creese B, Escott-Price V, *et al.* Proof-of-concept recall-by-genotype study of extremely low and high alzheimer's polygenic risk reveals autobiographical deficits and cingulate cortex correlates. *Alzheimers Res Ther* 2023;15:213.

## Supplementary methods

Cohort description .....	2
ABCD .....	2
IMAGEN.....	2
Generation R.....	2
ALSPAC .....	2
UK Biobank.....	3
Table 1. Cohort image acquisition and processing .....	4
Genetic data.....	6
Table 2. Information on genotyping and quality control.....	7
Genome-wide association studies .....	14
Alzheimer’s GWAS .....	14
Individual-level brain GWAS .....	14
Summary level brain GWAS .....	14
Two-sample Mendelian randomization.....	15
Harmonization of exposure and outcome GWAS data.....	15
Sensitivity analyses .....	15



## **Cohort description**

### ***ABCD***

The ABCD study (<http://abcdstudy.org>) consists of 11,875 participants of ages 9-10 years old at baseline. The aim of this study was to examine the effect of brain structure and function on developmental trajectories and addiction<sup>1</sup>.

### ***IMAGEN***

The IMAGEN study is a European multi-centre genetic neuroimaging study recruiting adolescents from secondary schools in London, Nottingham, Dublin, Paris, Berlin, Hamburg, Mannheim and Dresden. To ascertain a diverse sample with respect to socioeconomic status, emotional and cognitive development, private, state-funded and special schools were equally targeted. Participation in the study involves visits to the study centre and home assessments<sup>2</sup>.

### ***Generation R***

The Generation R study is a prospective population-based birth cohort from Rotterdam, the Netherlands. The aim of the Generation R Study is to identify genetic and environmental determinants that affect maternal and child development<sup>3</sup>. Study protocols were approved by the Medical Ethics Committee of the Erasmus Medical Center. All participants and their parents provided assent and informed consent, respectively.

### ***ALSPAC***

The Avon Longitudinal Study of Parents and Children (ALSPAC) is a prospective birth cohort which recruited pregnant women with expected delivery dates between April 1991 and December 1992 from Bristol UK<sup>4-6</sup>. The initial number of pregnancies enrolled is 14,541 and of these initial pregnancies, there was a total of 14,676 fetuses, resulting in 14,062 live births and 13,988 children who were alive at 1 year of age. When the oldest children were approximately 7 years of age, an attempt was made to bolster the initial sample with eligible cases who had failed to join the study originally. As a result, when considering variables collected from the age of seven onwards (and

potentially abstracted from obstetric notes) there are data available for more than the 14,541 pregnancies mentioned above. The total sample size for analyses using any data collected after the age of seven is therefore 15,454 pregnancies, resulting in 15,589 fetuses. Of these 14,901 were alive at 1 year of age. Between the ages of 18 to 21 years, a subset of ALSPAC offspring were invited to participate in three different neuroimaging studies: the ALSPAC-Testosterone study, the ALSPAC-Psychotic Experiences (PE) study, and the ALSPAC- Schizophrenia Recall by Genotype (SCZ-RbG) study. In total, MRI data was acquired for 958 participants: 513 in the Testosterone study, 248 in the Psychotic Experiences study and 197 in the ALSPAC-Schizophrenia Recall by Genotype study<sup>7</sup>. Please note that the study website contains details of all the data that is available through a fully searchable data dictionary and variable search tool (<http://www.bristol.ac.uk/alspac/researchers/our-data/>). Ethical approval for the study was obtained from the ALSPAC Ethics and Law Committee and the Local Research Ethics Committees. Informed consent for the use of data collected via questionnaires and clinics was obtained from participants following the recommendations of the ALSPAC Ethics and Law Committee at the time.

### **UK Biobank**

UK Biobank is a population-based study of 503,325 participants who were initially recruited from across Great Britain between 2006 and 2010, aged 40–69 years (<http://www.ukbiobank.ac.uk>). UK Biobank received ethical approval from the research ethics committee (REC reference 11/NW/0382). The present analyses were conducted under UK Biobank application number 48970.

**Table 1. Cohort image acquisition and processing**

Study sample	MRI-scanner	Software	Acquisition	Reference (PMID)	Quality control
The Adolescent Brain and Cognitive Development study (ABCD)	The ABCD imaging protocol is harmonized for three 3T scanner platforms (Siemens Prisma, General Electric (GE) 750 and Philips)	Freesurfer v5.3.0	<p><b>Siemens:</b> matrix=256x256, slices=176, FOV=256x256, % FOV phase=100%,Resolution (mm)=1.0x1.0x1.0, TR (ms)= 2000, TE (ms)=2.88, TI (ms)=1060, Flip Angle (deg)=8, Parallel Imaging=2x, MultiBand Acceleration=Off, Phase partial fourir=Off, Diffusion directions=N/A, b-values=N/A, Acquisition time=7:12</p> <p><b>Philips:</b> matrix=256x256, slices=225, FOV=256x240,% FOV phase=93.75%,Resolution (mm)=1.0x1.0x1.0, TR (ms)=6.31, TE (ms)=2.9, TI (ms)=1060, Flip Angle (deg)=8, Parallel Imaging=1.5x2.2, MultiBand Acceleration=Off, Phase partial fourir=Off, Diffusion directions=N/A, b-values=N/A, Acquisition time=5:38;</p> <p><b>General Electric:</b> matrix=256x256, slices=208,FOV=256x256, % FOV phase=100%,Resolution (mm)=1.0x1.0x1.0, TR (ms)= 2500, TE (ms)=2, TI (ms)=1060, Flip Angle (deg)=8, Parallel Imaging=2x, MultiBand Acceleration=Off, Phase partial fourir=Off, Diffusion directions=N/A, b-values=N/A, Acquisition time=6:09</p>	31415884	Removal of measures based on result of visual inspection
Avon Longitudinal Study of Parents and Children (ALSPAC)	3 Tesla General Electric HDx (GE Medical Systems) using an 8-channel head coil	Freesurfer v6.0.0	During each structural imaging session coronal T 1 scans were collected. Imaging parameters were as follows: 3D fast spoiled gradient echo (FSPGR) with 168–182 oblique-axial AC-PC sslices, 1 mm isotropic resolution; flip angle = 20°; repetition time (TR) = 7.9 ms; echo time (TE) = 3.0 ms; inverse time (TI) = 450 ms; 1mm × 1mm x 1mm voxel size; slice thickness 1 mm; FOV (field of view) 256 × 192 mm matrix. T 1- weighted scans took approximately 7.15 minutes each.	33043145	Removal of measures based on result of visual inspection
Generation R	3-Tesla MRI system (MR-750W, General Electric, Milwaukee, WI, US) using an eight-channel, receive-only	Freesurfer v6.0.0	High-resolution, T1-weighted structural MRI data were acquired using a coronal inversion recovery fast spoiled gradient recalled sequence with the following parameters: GE option BRAVO, TR = 8.77 ms, TE = 3.4 ms, TI = 600 ms, flip angle = 10°, matrix size = 220 × 220, field of view = 220 mm × 220 mm, slice thickness = 1 mm, number of slices = 230, ARC acceleration factor = 2.	29064008	Removal of measures based on result of visual inspection

head coil					
IMAGEN	3.0 T Philips Medical Systems Achieva; 3.0 T Brucker; 3.0 T Siemens TrioTim; 3.0 T Siemens Verio; 3.0 T Brucker/GE Medical Systems Signa Excite; 3.0 T GE Medical Systems Signa HDx	Freesurfer v5.3.0	Magnetic resonance imaging data were acquired at 8 European centers, using a standardised 3 Tesla, T1-weighted gradient echo protocol (voxel size=1.1 mm isotropic) based on that from the ADNI initiative ( <a href="http://adni.loni.usc.edu/methods/documents/mri-protocols/">http://adni.loni.usc.edu/methods/documents/mri-protocols/</a> )	21102431	No visual inspection of MRI images had been performed. We removed outliers 3 standard deviations above/below mean of respective measures.
UK Biobank	Siemens Skyra 3T running VD13A SP4, with a standard Siemens 32-channel RF receive head coil	Freesurfer v5.3.0	Voxel matrix: 1.0x1.0x1.0 mm - 208x256x256. 3D MPRAGE, TI/TR=880/2000 ms, sagittal orientation, in-plane acceleration factor=2	27643430, 29079522	No visual inspection of MRI images had been performed. We removed outliers 3 standard deviations above/below mean of respective measures.



## Genetic data

ALSPAC, IMAGEN, Generation R, and ABCD participants were genotyped using the Illumina HumanHap550, Illumina 610 and Illumina 660K, Illumina 670, and the Affymetrix NIDA SmokeScreen Array chips, respectively. For UK Biobank, the initial 50,000 participants were genotyped on Affymetrix UK BiLEVE Axiom array and the remaining 450,000 participants were genotyped using the Affymetrix UK Biobank Axiom<sup>®</sup> array and quad chip genotyping platforms. Details on quality control and imputation panels have been published elsewhere<sup>8</sup>. For ABCD, saliva samples were collected at baseline and sent to Rutgers University Cell and DNA Repository for storage and DNA isolation and genotyping was conducted using the Smokescreen array<sup>9</sup>. The initial dataset provided by the ABCD (ABCD\_release\_2.0.1\_r1) included 517,724 genetic variants chr1-23,25-26. For ABCD, we performed quality control using plinkQC and imputation of the genetic data using the Michigan imputation server. We identified individuals of European ancestry by combining the genotypes of ABCD with genotypes of 1000 genomes phase 3, consisting of individuals from known ethnicities. Principal component analysis using this genotype panel can be used to identify population structure down to the level of 1000 genomes (i.e. large-scale continental ancestry). To identify these individuals, we used check\_ancestry implemented in PLINK QC. It uses principal components 1 and 2 to find the centre of the European reference samples. We performed PCA analysis on the pruned ABCD dataset (Number of variants=152,094). All study samples whose euclidean distance from the centre falls outside a specified radius are considered non-European. We performed individual/sample-level quality control, as well as marker quality control. For each sample, the homozygosity rates across all X-chromosomal genetic variants were computed and compared with expected rates (females, X homozygosity<0.2); males, X chrom homozygosity>0.8). Samples with discordant sex information that is not accounted for were removed from the study. Outlying missing genotype and/or heterozygosity rates aids in detecting samples with poor DNA quality and/or concentration that should be removed from the study. We excluded individuals based a missing genotype rate of 3%, and individuals whose heterozygosity rate was 3 standard deviations above or below mean heterozygosity rate. For the marker-level quality control, we filtered genetic variants based on a Hardy Weinberg equilibrium exact test p value of 5e-07, a call rate of 95% and a minor allele frequency of 5%. In total, we retained 9,907 individuals (5,300 were of European ancestry) and 377,164 genetic variants. We performed imputation using the Michigan Imputation Server using hrc.r1.1.2016 reference panel, Eagle v2.3 phasing and multi-ethnic imputation process<sup>10</sup>. Code and further details can be found here [https://github.com/rskl92/ABCD\\_QC\\_genetic\\_data](https://github.com/rskl92/ABCD_QC_genetic_data).

**Table 2. Information on genotyping and quality control.**

Data type	Cohort/ source	HWE	MAF	Call Rate	Association	Imputation	Reference population	Genotype Platform
Individual-level data	ABCD	5.00E-07	0.01	0.95	Eagle2	minimac4	Haplotypes Reference Consortium (HRC)	Smokescreen array
	ALSPAC	5.00E-07	0.01	0.95	ShapeIT2	MACH 1.0.16 Markov Chain Haplotyping	1000 genomes phase 1 version 3 (release date 21/05/2011)	Illumina HumanHap550 quad
	Generation R	1.00E-07	0.001	0.9	mach	minimac?	1000 Genomes (phase 3; March 2012)	Illumina 610 and 660 K
	IMAGEN	1.00E-06	0.01	0.95	mach2qtl(1.1.2)	minimac (release 2012-05-29)	1000 Genomes (phase 1 version 3; Nov 2010)	Illumina 610-Quad and Illumina 660W-Quad
	UK Biobank	1.00E-06	>3% for info>0.3; info>0.6 for MAF 1-3%, info>0.8 for MAF 0.5-1%;info>0.9 for MAF 0.1-0.5%	0.95	SHAPEIT2	impute2	Haplotypes Reference Consortium (HRC) and UK10K haplotype	UK Biobank Axion Array
Summary-level data for subcortical structures	ENIGMA consortium; Satizabal, Hibar, and Adams	See respective publication <sup>11-13</sup>	See respective publication <sup>11-13</sup>	See respective publication <sup>11-13</sup>	See respective publication <sup>11-13</sup>	See respective publication <sup>11-13</sup>	See respective publication <sup>11-13</sup>	See respective publication <sup>11-13</sup>
Summary-level data for cortical measures	ENIGMA consortium; Grasby et al	See respective publication <sup>14</sup>	See respective publication <sup>14</sup>	See respective publication <sup>14</sup>	See respective publication <sup>14</sup>	See respective publication <sup>14</sup>	See respective publication <sup>14</sup>	See respective publication <sup>14</sup>

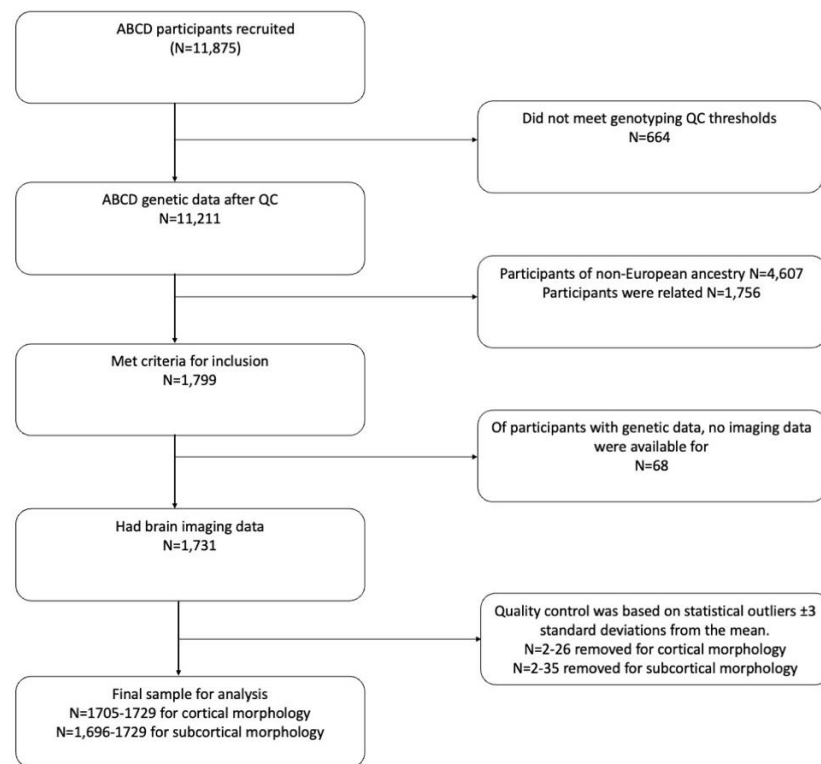


**Figure 1a.** Flow chart representing inclusion into the study sample for ABCD included in the childhood meta-analysis.

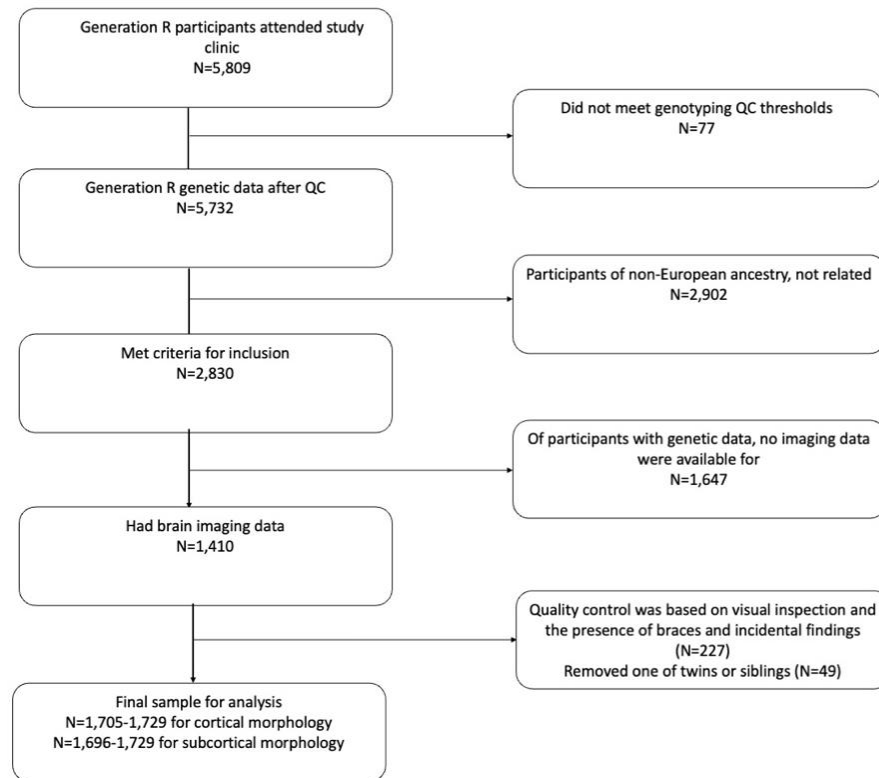


**Figure 1b.** Flow chart representing inclusion into the study sample for Generation R included in the childhood meta-analysis.



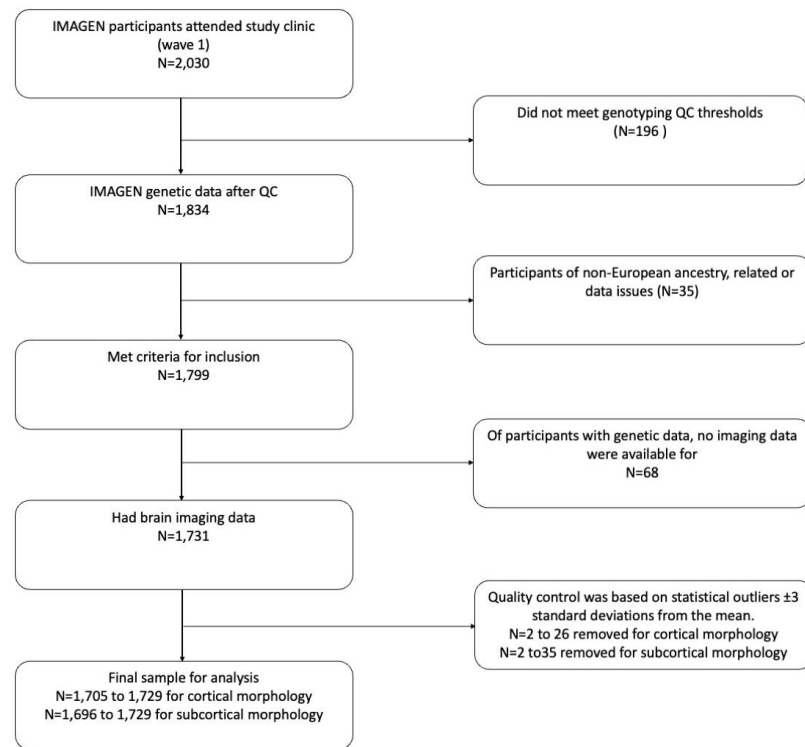


**Figure 1c.** Flow chart representing inclusion into the study sample for IMAGEN (wave 1) included in the childhood meta-analysis.

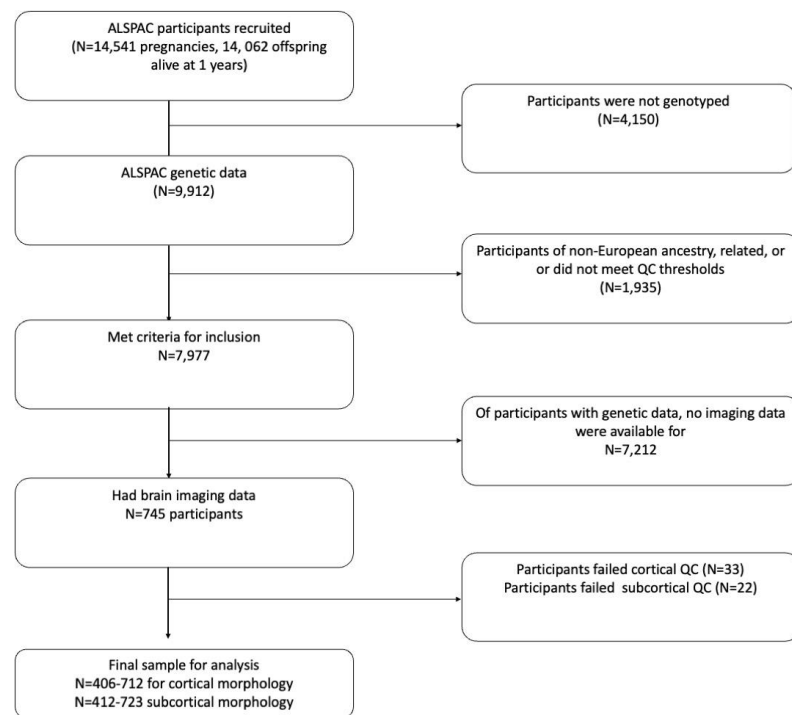


**Figure 2a.** Flow chart representing inclusion into the study sample for ALSPAC included in the early adulthood meta-analysis.

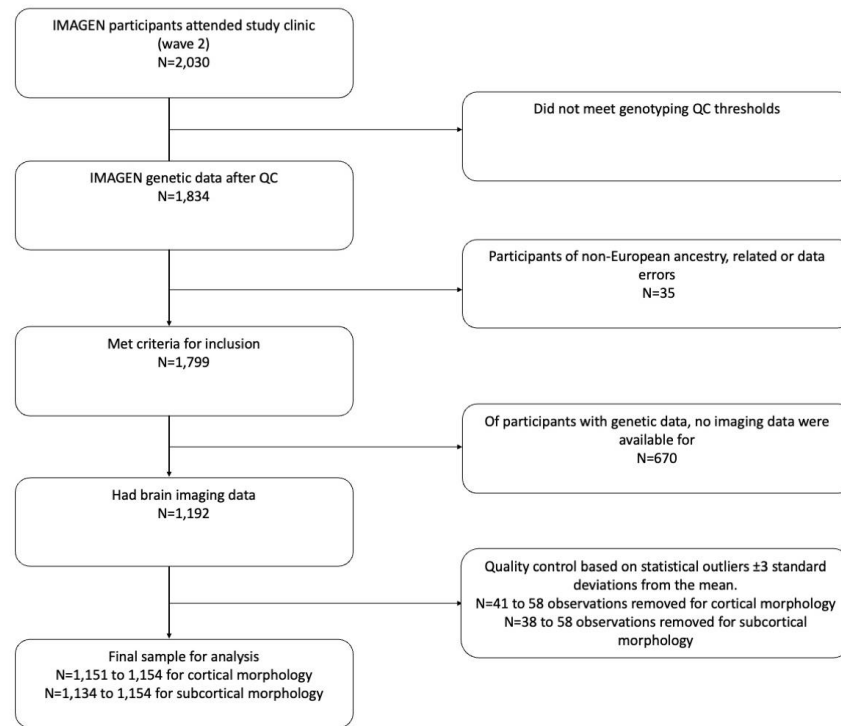


**Figure 2b.** Flow chart representing inclusion into the study sample for IMAGEN (wave 2) included in the early adulthood meta-analysis.

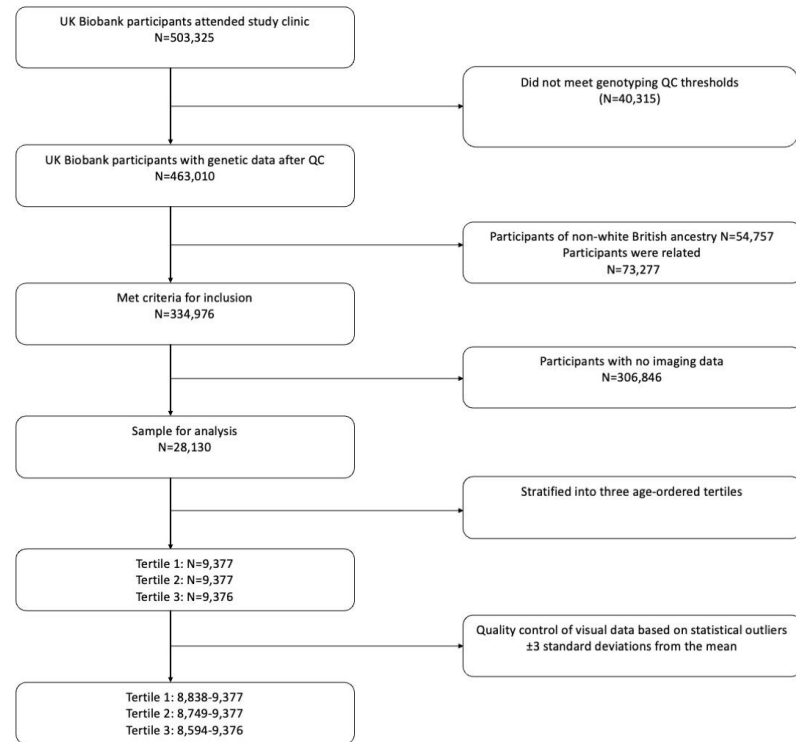


**Figure 3.** Flow chart representing inclusion into the study sample for UK Biobank (adulthood sample).

## Genome-wide association studies

### **Alzheimer's GWAS**

International Genomics of Alzheimer's Project (IGAP) is a large three-stage study based upon genome-wide association studies (GWAS) on individuals of European ancestry. In stage 1, IGAP used genotyped and imputed data on 11,480,632 single nucleotide polymorphisms (SNPs) to meta-analyse GWAS datasets consisting of 21,982 Alzheimer's disease cases and 41,944 cognitively normal controls from four consortia: The Alzheimer Disease Genetics Consortium (ADGC); The European Alzheimer's disease Initiative (EADI); The Cohorts for Heart and Aging Research in Genomic Epidemiology Consortium (CHARGE); and The Genetic and Environmental Risk in AD Consortium Genetic and Environmental Risk in AD/Defining Genetic, Polygenic and Environmental Risk for Alzheimer's Disease Consortium (GERAD/PERADES). In stage 2, 11,632 SNPs were genotyped and tested for association in an independent set of 8,362 Alzheimer's disease cases and 10,483 controls. Meta-analysis of variants selected for analysis in stage 3A (n = 11,666) or stage 3B (n = 30,511) samples brought the final sample to 35,274 clinical and autopsy-documented Alzheimer's disease cases and 59,163 controls.

### **Individual-level brain GWAS**

We retained only individuals of European ancestry from all cohorts used in our analysis. In ALSPAC, IMAGEN, Generation R, and UK Biobank we included unrelated individuals.

We estimated the effects of the Alzheimer's disease genetic variants on each standardised brain structure in individuals of European ancestry, using the `lm` function in RStudio version 3.3.1, for ALSPAC, IMAGEN, Generation R, and UK Biobank. The models for all cohorts were adjusted for age, sex, and ancestry-derived principal components. For ABCD, we used BOLT-LMM version 2.3 (linear mixed model (LMM)) software. BOLT-LMM applies an LMM to examine the association between genetic variants and phenotypes, whilst accounting for population stratification and cryptic relatedness<sup>15</sup>. For ALSPAC, IMAGEN, and Generation R, we adjusted for five genetic principal components. For ABCD and UK Biobank, we adjusted for ten genetically informative principal components.

### **Summary level brain GWAS**

Summary statistics of cortical thickness and subcortical volumes were obtained from the ENIGMA consortium<sup>11–13</sup>. The GWAS by Satizabal et al<sup>11</sup> were based on brain MRI scans and genome wide genotype data of up to 37,741 individuals from ENIGMA, CHARGE, and UK Biobank. GWAS for



hippocampal volume<sup>12</sup> and estimated total intracranial volume<sup>13</sup> were based on the brain MRI images of 33,535 and 37,345 participants, respectively, from the ENIGMA and CHARGE consortia. The meta-analyses of global and regional thickness of 34 cortical regions consisted results from 33,992 participants from ENIGMA and UK Biobank<sup>14</sup>. All cortical regions and subcortical structures were mapped to the Desikan-Killiany atlas<sup>16</sup>. All participants in these studies provided written informed consent and sites involved obtained approval from local research ethics committees or Institutional Review Boards.

### **Two-sample Mendelian randomization**

#### ***Harmonization of exposure and outcome GWAS data***

Only biallelic single nucleotide polymorphisms (SNPs) were included as instruments (insertions and deletions were removed). SNPs for each Alzheimer's SNP was identified in the brain GWAS. Proxies were identified for any SNPs not found ( $r^2 > 0.8$  using 1000 genomes as a reference). Proxies may differ between datasets. In a two-sample MR analysis, the effect of a SNP on exposure and an outcome must be harmonised relative to the same allele. SNPs for the exposure were coded such that the effect allele was always the 'increasing allele' (e.g. allele increasing Alzheimer's disease when examining genetic liability for Alzheimer's disease on brain structures or the allele increasing brain structure in the reverse direction of the bidirectional analysis), and the alleles were harmonized so that the effect on the outcome corresponded to the same allele as the exposure.

#### ***Sensitivity analyses***

A range of sensitivity analyses were conducted to check for violation of the key MR assumptions and check the robustness of the causal effect estimates:

(1) The inverse variance weighted (IVW) method assumes no horizontal pleiotropy (i.e. it assumes there are no causal paths from the SNPs to brain structures that do not go through Alzheimer's disease)<sup>17</sup>. It also assumes the gene-exposure association estimates are measured with no measurement error (NOME assumption)<sup>17</sup>. Thus, we compared effect estimates from the IVW regressions to those obtained with MR-Egger regression models, as the use of many alleles in MR analyses increases the potential for pleiotropic effects due to aggregation of invalid genetic instruments<sup>18</sup>. MR-Egger assumes NOME but relaxes the assumption that the effects of genetic variants on the outcome operate entirely via the exposure (i.e. no horizontal pleiotropy), by not constraining the intercept term to zero in the weighted regression described above. In this instance,

the intercept parameter estimates the overall pleiotropic effect of the SNPs on the outcome, with a non-zero intercept providing evidence for bias due to pleiotropy. The *beta* coefficient (or slope) of MR-Egger provides a causal estimate of the exposure on the outcome, accounting for this level of pleiotropy and assuming that the pleiotropic effect of SNPs on the outcome is not correlated with the instrument strength.

(2) We compared the results from IVW and MR-Egger regression to those obtained with the weighted median method<sup>19</sup>, which provides a consistent estimate of causal effect if at least 50% of the genetic variants are valid instrumental variables (i.e. robustly associated with the exposure, not associated with confounding factors and only associated with the outcome via the exposure of interest). The weighted mode method assumes that the plurality of genetic variants are valid instrumental variables<sup>20</sup>. (4) The presence of excessive between-SNP heterogeneity in an MR analysis may indicate that some of the genetic variants are pleiotropic. Thus, we assessed heterogeneity (i.e. variability in estimates from different genetic variants) using Cochran's Q statistic<sup>17</sup>.

(3) In MR, it is assumed that the genetic instruments influence the exposure first and then the outcome, through the exposure. However, it is possible that the SNPs used to instrument structural brain measures may have a direct effect on AD risk, which then goes on to influence structural brain measures. To test that the hypothesised causal direction was correct for each SNP, we performed directionality tests which investigate whether the SNP explains more variance in the exposure than it does in the outcome (which should be true if the hypothesised causal direction from exposure to outcome is correct)<sup>21</sup>.

**References:**

1. Casey, B. J. *et al.* The Adolescent Brain Cognitive Development (ABCD) study: Imaging acquisition across 21 sites. *Developmental Cognitive Neuroscience* **32**, 43–54 (2018).
2. Schumann, G. *et al.* The IMAGEN study: Reinforcement-related behaviour in normal brain function and psychopathology. *Molecular Psychiatry* **15**, 1128–1139 (2010).
3. White, T. *et al.* Pediatric population-based neuroimaging and the Generation R Study: The intersection of developmental neuroscience and epidemiology. *Eur. J. Epidemiol.* **28**, 99–111 (2013).
4. Fraser, A. *et al.* Cohort Profile: the Avon Longitudinal Study of Parents and Children: ALSPAC mothers cohort. *Int. J. Epidemiol.* **42**, 97–110 (2013).
5. Boyd, A. *et al.* Cohort Profile: the 'children of the 90s'--the index offspring of the Avon Longitudinal Study of Parents and Children. *Int. J. Epidemiol.* **42**, 111–127 (2013).
6. Northstone, K. *et al.* The Avon Longitudinal Study of Parents and Children (ALSPAC): an update on the enrolled sample of index children in 2019 [version 1; peer review: 2 approved]. *Wellcome Open Res.* (2019). doi:10.12688/wellcomeopenres.15132.1
7. Sharp, T. H. *et al.* Population neuroimaging: generation of a comprehensive data resource within the ALSPAC pregnancy and birth cohort. *Wellcome Open Res.* (2020). doi:10.12688/wellcomeopenres.16060.1
8. Bycroft, C. *et al.* Genome-wide genetic data on ~500,000 UK Biobank participants. *doi.org* 166298 (2017). doi:10.1101/166298
9. Baurley, J. W., Edlund, C. K., Pardamean, C. I., Conti, D. V. & Bergen, A. W. Smokescreen: A targeted genotyping array for addiction research. *BMC Genomics* (2016). doi:10.1186/s12864-016-2495-7
10. Das, S. *et al.* Next-generation genotype imputation service and methods. *Nat. Genet.* **48**, 1284–1287 (2016).
11. Satizabal, C. L. *et al.* Genetic architecture of subcortical brain structures in 38,851 individuals. *Nat. Genet.* (2019). doi:10.1038/s41588-019-0511-y
12. Hibar, D. P. *et al.* Novel genetic loci associated with hippocampal volume. *Nat. Commun.* **8**, 13624

- (2017).
13. Adams, H. H. H. *et al.* Novel genetic loci underlying human intracranial volume identified through genome-wide association. *Nat. Neurosci.* **19**, 1569–1582 (2016).
  14. Grasby, K. L. *et al.* The genetic architecture of the human cerebral cortex. *Science (80-. )*. **367**, eaay6690 (2020).
  15. Loh, P. R., Kichaev, G., Gazal, S., Schoech, A. P. & Price, A. L. Mixed-model association for biobank-scale datasets. *Nat. Genet.* **50**, 906–908 (2018).
  16. Desikan, R. S. *et al.* An automated labeling system for subdividing the human cerebral cortex on MRI scans into gyral based regions of interest. *Neuroimage* **31**, 968–980 (2006).
  17. Bowden, J., Davey Smith, G. & Burgess, S. Mendelian randomization with invalid instruments: Effect estimation and bias detection through Egger regression. *Int. J. Epidemiol.* **44**, 512–525 (2015).
  18. Haycock, P. C. *et al.* Best (but oft-forgotten) practices: The design, analysis, and interpretation of Mendelian randomization studies. *American Journal of Clinical Nutrition* **103**, 965–978 (2016).
  19. Bowden, J., Davey Smith, G., Haycock, P. C. & Burgess, S. Consistent Estimation in Mendelian Randomization with Some Invalid Instruments Using a Weighted Median Estimator. *Genet. Epidemiol.* (2016). doi:10.1002/gepi.21965
  20. Hartwig, F. P., Smith, G. D. & Bowden, J. Robust inference in summary data Mendelian randomization via the zero modal pleiotropy assumption. *Int. J. Epidemiol.* (2017). doi:10.1093/ije/dyx102
  21. Hemani, G., Tilling, K. & Davey Smith, G. Orienting the causal relationship between imprecisely measured traits using GWAS summary data. *PLoS Genet.* **13**, (2017).